International Journal of Engineering Trends and Technology
ISSN: 2231–5381 / https://doi.org/10.14445/22315381/IJETT-V74I2P102

Volume 74 Issue 2, 19-41, February 2026

Original Article

Optimization and Simulation of a Solar Flat Plate Collector Using Response Surface Methodology and Computational Fluid Dynamics

Vivek G[1], Lakshmipathy B[2], Ramesh P[3], Manivannan M[4]

[1,3]*Department of Mechanical Engineering, Annamalai University, Chidambaram, Tamil Nadu, India.*
[2]*Department of Mechanical Engineering, Annamalai University, Chidambaram, Tamilnadu, India, and Government Polytechnic College, Kadathur, Dharmapuri, Tamilnadu, India.*
[4]*Department of Electronics & Instrumentation Engineering, Annamalai University, Chidambaram, Tamil Nadu, India.*

[1]*Corresponding Author : anandanvivek580@gmail.com*

Received: 03 November 2025 Revised: 09 January 2026 Accepted: 11 January 2026 Published: 14 February 2026

Abstract *- Solar collector technology has just taken a step forward to ensure that the thermal energy requirements of society are addressed. Development of solar thermal technologies has necessitated the need to employ both computational and experimental tools in an effort to optimise the performance of the system. The paper presents a holistic approach to optimising the thermal efficiency of solar flat plate collectors using Response Surface Methodology (RSM) and Computational Fluid Dynamics (CFD). Box-Behnken experimental design has been applied to determine the effects of main parameters, comprising mass flow rate, angle of inclination, and secondary riser inclination, on water outlet temperature. The thermal performance of both optimised and baseline designs was legitimised by CFD simulations. Findings have shown that CFD and RSM models are closely correlated with each other, and outlet temperature prediction has a low deviation of 0.167 K, which emphasizes the precision of the regression model. The highest thermal efficiency was recorded at secondary riser inclination of 11.141, mass flow rate of 23.628 kg/h, inclination angle of 7.226, which gave an outlet temperature of 351.448 K with a desirability score of 1.000. This CFD-RSM system is a powerful and affordable approach to optimization of solar collector designs, and helps to mitigate the need for large-scale experimental studies heavily, and offers scalable solutions to future solar thermal utilizations.*

Keywords *- Computational Fluid Dynamics (CFD), Outlet Temperature, Renewable Energy, Response Surface Methodology (RSM), Solar Flat Plate Collector, Thermal Optimization.*

1. Introduction

The solar flat plate collector systems have become a significant part of the Emerging renewable energy technologies, which are a sustainable and environmentally acceptable source of alternative heating means to the conventional ones. Due to their simplicity, low cost, and absence of complexities to install, these systems are widely applied in residential and industrial settings to minimize the use of energy and correction of carbon emissions.

Solar thermal heating systems, specifically solar air heaters and flat plate solar water heating systems, are central to the increased use of renewable energy sources as well as the need to meet the rising energy consumption needs around the world, rigorously reducing greenhouse gas emissions. However, despite these benefits, the overall performance of flat plate collectors is very sensitive to a number of critical design and operating parameters such as riser tube inclination, mass flow rate, absorber tilt angle, and flow configuration. Those parameters make thermal performance very sensitive. Hence, optimization methods complex enough to reflect the intricate interaction of these parameters should be adopted.

Traditional trial-and-error design methodologies are usually unable to determine the nonlinear interactions between heat transfer and fluid flow in the collector. In this regard, the current development of electronic and statistical optimization methods has made significant breakthroughs in the research and development of solar thermal systems. Computational Fluid Dynamics (CFD) has emerged as an essential means of offering a greater understanding of fluid flow, temperature, and heat transfer processes, making it a high-fidelity thermo-hydraulic model of collector design. Simultaneously, Response Surface Methodology (RSM) provides a predictably structured and computationally cost-effective approach to performing the analysis of the inherent and interactive impacts of a variety of design and operating variables, which allows creating models to forecast performance.

The combination of CFD and RSM has been shown to work exceptionally well in the field of solar thermal research, with the results of CFD being physically accurate. In contrast, RSM can be used to provide a strong statistical model and optimization at a lower level of computation. Such a combined strategy offers a solid basis for improving the effectiveness of solar water heaters and other thermal systems by establishing optimal parameter combinations and tracking their performance trends. Nevertheless, there remains an enduring challenge of achieving high thermal efficiency and high heat transfer, with effective flow resistance and related hydraulic penalties observed to accompany the latter. Therefore, the necessity to conduct additional studies devoted to new collector designs and combined optimization strategies that are able to provide a balance between thermal improvement and reasonable flow properties is evident.

2. Review of Literature

The research on solar thermal collectors indicates a developmental advancement from simplistic theoretical studies to complex design models based on optimization and numerical and experimental confirmations. The pioneering work defined the core principles of solar thermal systems, including collector types, heat transfer, and areas of application. Extensive reviews have indicated a primary role of absorber design, flow configuration, material properties, and thermal loss mechanisms as the determining factor of the thermal performance of flat plate and air-based collectors, thus laying the groundwork to further performance improvement studies (Kalogirou, 2004; Jaisankar & Ananth, 2011; Pandey and Chaurasiya, 2017; Sadhishkumar and Balusamy, 2014).

As the computational resources available have improved, Computational Fluid Dynamics (CFD) has become one of the key analysis tools in the study of the behavior of heat transfer and fluid flow in solar collectors. Initial validation-oriented studies showed that the CFD predictions were in good accord with the experimental data, proving that the numerical models could be successfully used in the steady-state and transient study of flat plate solar water heating systems (Reichl et al., 2015; Gunjo et al., 2017). Later studies used CFD to study the distribution of temperature, the velocity fields, and the convective heat transfer coefficients to understand the inner thermal-hydraulic process of collectors at different operating conditions in detail (Junaid et al., 2017; Soundararajan and Sugan, 2015). Extended literature also highlighted CFD's capability to handle complex geometry, turbulence, and conjugate heat transfer, which supports its application as a diagnostic and design forecasting tool (Bhutta et al., 2012; Anil Singh Yadav and Bhagoria, 2013).

One significant body of research has focused on geometric modification and flow disturbance methods to improve convective heat transfer. This has been demonstrated with the introduction of the baffles, fins, corrugations, protrusions, and inclined flow elements, which have been observed to enhance turbulence and thermal performance. It was numerically proved that semi-circular baffles and corrugated absorber plates contribute significantly to the improvement of heat transfer because they raise the fluid mixing and residence time (Thejaraju et al., 2017; Hussen and Zeru, 2020). Newer designs used more complicated geometries, including protrusions of a frustum shape and zig-zag tubes, and found significant thermal efficiency improvements by optimizing these designs with multi-objective methods (Wang et al., 2024; Korti et al., 2023). Nevertheless, these improvements are often accompanied by a higher pressure drop, which is why the trade-off between thermal gains and hydraulic penalties is of great significance.

The use of advanced working fluids and especially nanofluids is another method that has been found effective in enhancing the performance of solar collectors. Both experimental and numerical studies have consistently shown that nanofluids exhibit enhanced heat transfer properties due to their higher thermal conductivity compared to the base fluids (Desisa et al., 2023). More recent works took this even further, introducing hybrid nanofluids and investigating their thermomagnetic convection behavior using response surface methodology, demonstrating enhanced predictive capability and potential for performance optimization (Ben Said et al., 2024). Along with these advantages, several authors highlight unaddressed issues of long-term stability, higher pumping power, and economic viability, suggesting the need to conduct combined thermo-economic and durability evaluations (Vyas et al., 2024).

Concurrently, there has been exploration of hybrid and integrated solar thermal systems that enhance the comprehensive use of energy and the system's flexibility. People have experimentally studied the hybrid solar air heaters and building-integrated collector storage systems and found that two heat transfer modes or the combination of collectors with complementary systems could be more efficient in energy use and space utilization (Potgieter et al., 2020; Garnier et al., 2018). System-level explorations, such as active solar water heating systems and solar-assisted energy systems, also show that operational approaches and integration are a decisive factor to define real-world performance in addition to component-level optimization (Gong and Sumathy, 2016; Woyessa et al., 2020).

The optimization methodologies have become an integral part of modern research in solar thermal. Response Surface Methodology (RSM) has become very popular to establish complex parametric relationships and determine optimal design and operating conditions at low computational cost (Qader et al., 2019; Omo-Oghogho and Aliu, 2020; Kazemian and Khosravi, 2025). Besides, multi-objective optimization models have been used to optimize the competing goals of thermal efficiency, pressure drop, and entropy generation in order to offer more realistic and balanced design solutions

(Wang et al., 2024). Combining CFD and Design of Experiments (DOE) can make it even stronger and more predictive, which has already been proven in recent thermal systems optimization works (Choi et al., 2025; Varma Kola et al., 2021).

Within the context of emerging digital trends, including Building Information Modeling (BIM), Artificial Intelligence (AI), and the Internet of Things (IoT), the recent literature highlights an increasing focus on data-driven monitoring, predictive control, and system-level optimization of solar power systems. The high-dimensional design space and real-time operational model decision-making with AI-driven algorithms and sophisticated optimization methods are actively studied to use in the case of multi-objective energy systems. The use of IoT-based solar thermal systems has been mentioned in relation to performance measurement, adaptive control, and connection with intelligent energy networks, which allows a solar thermal system to obtain real-time data acquisition and operational optimization on the system level (Gong and Sumathy, 2016). Although Building Energy Modeling (BEM) is more common, the studies that are BIM-oriented are more focused on the entire integration of solar thermal elements into building envelopes and the evaluation of their lifecycle performance (Garnier et al., 2018).

It is in this context that the current methodology, based on the optimization and simulation of a solar flat plate collector with the RSM within a CFD framework, provides a strong, physics-based alternative to data-only AI or IoT-based schemes. The CFD-RSM method directly obtains the underlying physical processes in heat transfer and fluid flow, and allows systematic parametric optimization at low computational cost, unlike AI-based models, which may have large operating data sets and, in many cases, are not physically interpretable. In comparison to the BIM- and IoT-based frameworks, which are mainly used to target the system integration and operational monitoring, the current methodology focuses on component-level thermal-hydraulic optimization during the design phase, thus enhancing (but not eliminating) the digital energy management strategies. The given positioning emphasizes the applicability of the CFD-aided optimization of RSM as a good and transparent design process, especially in conditions where there are not enough experimental data available and extra knowledge about the mechanisms of performance improvement is needed.

In addition to the first-law efficiency analysis, second-law and sustainability-based metrics are gaining increasing focus following recent studies. The irreversibility and the general quality of the system have been estimated by the minimization of entropy generation and exergy-based evaluations, which show that some methods of thermal enhancement can enhance the efficiency at the same time increasing irreversibility unless optimized well (Abrofarakh et al., 2024). The supporting enviro-economic analyses emphasize the fact that solar thermal systems need to be assessed based on environmental impact and cost-effectiveness, as well as thermal performance (Prabhu & Vengadesan, 2024).

On the whole, the observed shift in the literature toward CFD-, optimization-, and sustainability-based design of solar thermal collectors. Although AI-, BIM-, and IoT-based models are increasingly becoming popular in smart operation and system integration, CFD-based RSM optimization is one of the most important and trustworthy approaches to the design-level improvement of the solar flat plate collectors. The combination of these complementary paradigms, which is facilitated by experimental tests and exergy-based evaluation, can be seen as a promising field in future research to create scalable, intelligent, high-performance solar thermal systems.

2.1. Problem Definition

It is made clear in the literature that current solar thermal studies have been based on constructive modeling models, especially in the testing and optimization of water-based flat plate wash as a method of water-based flat plate collector validation with integrated CFD-RSM models (Abrofarakh & Moghadam, 2024; Ben Said et al., 2024). Previous literature shows that important design and operating factors such as the secondary riser inclination, the collector tilt angle, and the mass flow velocity have a substantial impact on the heat transfer performance and thermal efficiency. CFD and RSM have been applied to enable systematic searches over complex multivariable design spaces, with efficiency gains of up to 35 reported, and the promise of optimized solar thermal systems for addressing energy and environmental problems is demonstrated. Based on these results, the current work highlights the optimization and performance analysis of a solar flat plate collector using a coupled CFD-RSM model. The new aspect is the smooth combination of high-fidelity CFD-based thermo-fluid analysis with a statistically sound RSM model to fully capture the interactions between parameters and determine the optimum design and operating conditions, which enhances the predictability, practical extrapolation, and scalability of the optimized collector designs to real-world applications.

3. Methodlogy

This study is an integrated Computational Fluid Dynamics (CFD) and Response Surface Methodology (RSM) study, which is used to optimize and test the thermal efficiency of a solar flat plate collector systematically. An experimentally tested three-dimensional numerical simulation of a conjugate heat transfer model is created with experimentally tested geometric and material specifications. The important operational and geometric parameters, such as mass flow rate, secondary riser inclination, and collector inclination, are manipulated to statistically configure design space determined by a Box Behnken experimental design (Wang et al., 2023). Transient CFD simulations are conducted to follow the thermal evolution and steady-state behaviour,

and numerical accuracy is ensured through grid independence tests and strict convergence criteria. The quadratic regression models based on the RSM approach capture parameter interactions and can predict outlet temperature. The cross-validation of the CFD results, statistical prediction, and experimental data indicates high accuracy and reproducibility. The combined approach will help provide a credible performance optimization with a smaller amount of experimental effort and high relevance to real-world solar flat plate collector design.

3.1. Geometric and Operational Parameters

The display experimental model with fixed shapes and sizes. It contains external and internal diameters of header pipe, primary and secondary riser pipes, angle of the secondary riser, size of absorber plate, and material (copper). The fluid was water with an initial pressure of 1.01325 bar and an inlet temperature of 307 K. The Mass flow rate has been kept at 23.628 kg/h.

Figure 1 presents a simple design for a flat-plate solar collector. This comprises 2 header tubes placed horizontally at the top and bottom, joined together with 9 vertical pipes called risers. The intake of the bottom header tube is where cold water flows. Fluid receives heat from solar radiation incident on the collector's absorber surface as it flows up through the risers. Hot fluid finally exits through the outlet at the top of the header tube. Such construction leads to adequate circulation and heat absorption as risers effectively convey heat to the flow of water inside. Header tubes serve as distributors, which provide an equal flow of water in all riser pipes. The design is widely applied in home and industrial solar water heating systems as it is straightforward, reliable, and inexpensive.

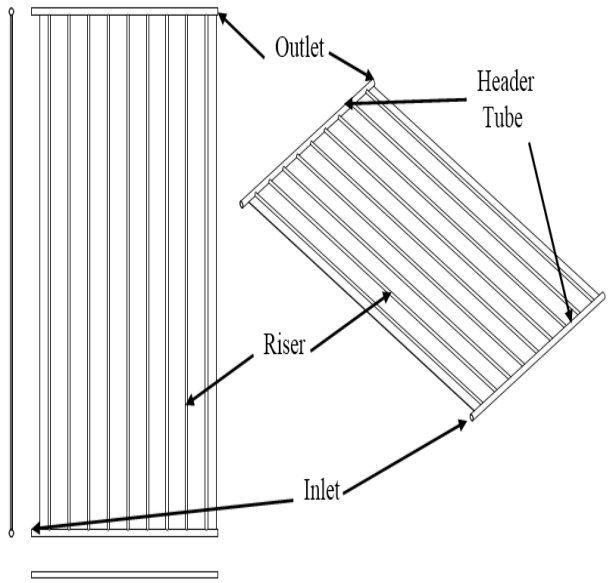

Fig. 1 Base model of the solar collector system

Table 1. Geometry conditions

Parameter	Specifications
Angle of secondary riser inclination	11.141 deg
Distance between risers	0.120 m
Fluid	Water
Initial Pressure	1.01325bar
Inlet water temperature	307 K
Inner diameter of header pipes	0.025 m
Inner diameter of Primary and Secondary riser Pipes	0.012 m
Length of absorber plate	1.970 m
Length of Riser pipes	1.9885 m
Mass Flow Rate	23.628 Kg/h
Outer diameter of header Pipes	0.028 m
Outer diameter of Primary and Secondary riser Pipes	0.015 m
Solid	Copper
Thickness of absorber plate	0.003 m
Width of absorber	1.080 m

3.2. Boundary Conditions

Tables 2 to 4 contain extensive data on boundary conditions, initial conditions, and numerical parameters required to perform a CFD simulation of a solar flat plate collector.

Table 2. Boundary surface region definitions

Boundary Surface	Region Definition
Absorber plate top	Solid
Absorber Plate Bottom	
Fluid-solid interface	Forward: Fluid
	Reverse: Solid
Inflow	Fluid
Insulation	
Outflow	

Table 3. Region parameters

Parameter	Region	
	Fluid	Solid
Temperature (K)	326	351
Pressure (Pa)	101325	NA
Turbulent Kinetic Energy (m^2/s^2)	1.0	NA
Turbulent Dissipation Rate (m^2/s^3)	100	NA
Species	H_2O	Copper

Effective heat transfer modelling requires boundary surfaces, as defined in Table 2 (fluid-solid interfaces and insulation boundaries). Table 3 determines starting area parameters by assigning unique values of temperature, pressure, and turbulence to Fluid (Water) and Solid (Copper) Domains, and gives a realistic starting point to simulation analyses. Lastly, Table 4 specifies the solver configuration,

convergence criteria, and iterative settings intended to solve complex momentum, pressure, density, energy, and turbulence equations quickly and accurately, while remaining numerically stable and accurately representing the solution. Collectively, these tables provide a methodological basis for robust, reliable simulation results.

Table 4. Solver parameter for equations

Parameter	Momentum	Density	Pressure	Turbulent Kinetic Energy	Energy	Turbulent Dissipation Rate
Solver Type	SOR	SOR	HYPRE BICGSTAB	SOR	SOR	SOR
Convergence Tolerance	1e-05	1e-04	1e-06	1e-03	1e-04	1e-03
Minimum Iterations	0	2	2	2	2	2
Maximum Iterations	50	20	5000	50	20	50
SOR Relaxation	1.0	1.0	1.1	0.7	1.0	0.7

3.3. Gird Independence Test

Figure 2 demonstrates variations in outlet water temperature of the solar collector system with time, real conditions versus numerical models with absorber plate thicknesses of 4-6 mm. At first, the outlet temperature rises slowly, reaching a peak at 8,000-10,000 seconds, after which it tends to decrease. In all simulations, a 6 mm thickness yields the highest output temperature, indicating better thermal retention and improved heat transfer efficiency. On the other hand, the lowest temperatures were obtained with a 4 mm thickness, indicating low thermal performance. The experimental results are close to the 5 mm simulation results, indicating that the numerical model is accurate at this thickness. In general, studies indicate that with greater absorber plate thickness, the solar collector becomes more thermally efficient; however, in practice, issues of cost and practicality must be taken into account when choosing the design.

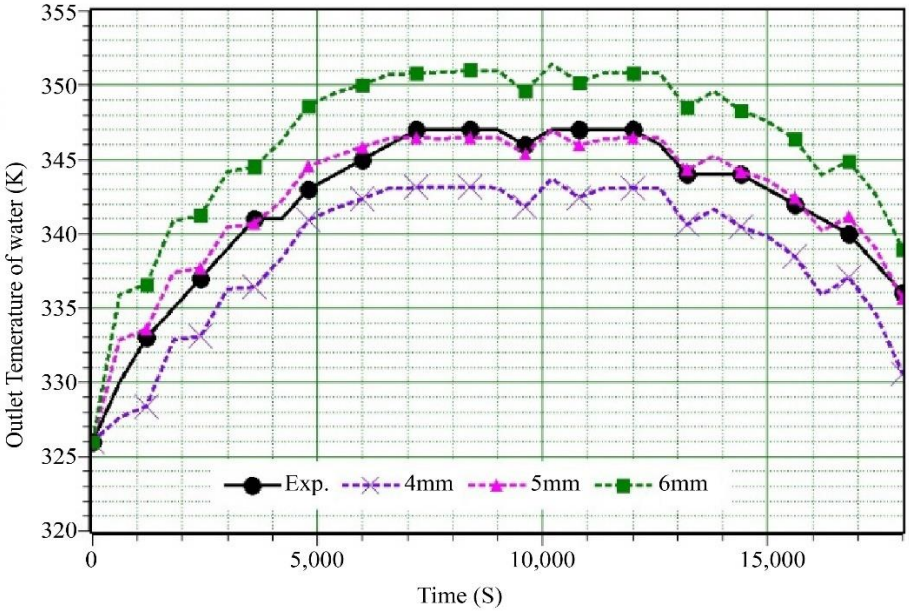

Fig. 2 Validation and grid independence study of CFD simulation

4. Response Surface Methodology Analysis

This study employs RSM to discuss how 3 critical design parameters influence the outlet temperature of a solar flat plate collector, which includes the angle of secondary riser inclination, mass flow rate, and angle of inclination. The ongoing investigation employs the Box-Behnken experimental methodology, which has identified optimal parameter combinations for maximum thermal performance. The range of 3 critical elements that were measured in this study, according to Table 5, includes angle of secondary riser inclination (10°-80°), mass flow rate (5.6-25.6 kg/h), and angle of inclination (6°-16°). These clearly specified parameter ranges provide a formal understanding of their respective and combined effects on the collector's output temperature, enabling complete optimization of the solar flat plate collector design.

Table 5. RSM of Box-Behnken DESIGN

S.No	Name of the factor	Minimum	Maximum
1	Angle of secondary risers inclination (deg)	10	80
2	Angle of inclination (deg)	6	16
3	Mass flow rate (kg/h)	5.56	25.55

The normalised results of 3 selected design elements, namely, Secondary Riser Inclination (A), Mass Flow Rate (B), and Angle of Inclination (C), are presented in Table 6.

It also displays normalised responses of outlet temperature that accompany each of these factors. Normalisation was performed as an essential step in the Box-Behnken design of experiments to place all variables and responses within the range of -1 and 1. This will ensure all variables are treated equally in the regression model, regardless of their initial units or size.

The table explicitly shows the distribution of design points for each factor at the low (–1), medium (0), and high (+1) levels. Mass flow rates of 5.6, 15.6, and 25.6 kg/h are also represented with secondary riser inclination of 10° as -1, 45° as 0, and 80° as +1. RSM model subsequently applies normal responses to develop quadratic regression equations that coincide with the measured outlet temperature at every design combination. Besides simplifying statistical analysis, this systematic coding demonstrates the impact of each element on performance, relative to others.

Table 6. Design factors and normalized responses

Run	Surface			Response
	Angle of secondary risers inclination (deg)	Mass flow rate (kg/h)	Angle of inclination (deg)	Outlet temperature (K)
1	80	25.55	11	348.6951
2	10	15.56	6	351.2028
3	45	5.6	16	337.0651
4	45	15.6	11	345.446
5	10	5.6	11	339.653
6	80	15.6	16	343.840
7	80	15.6	6	349.6554
8	45	15.6	11	345.446
9	10	25.6	11	348.8109
10	45	15.6	11	345.446
11	45	25.6	16	347.2351
12	45	15.6	11	345.446
13	45	5.6	6	341.2765
14	80	5.6	11	341.31765
15	45	25.6	6	350.343
16	45	15.6	11	345.446
17	10	15.6	16	345.6381

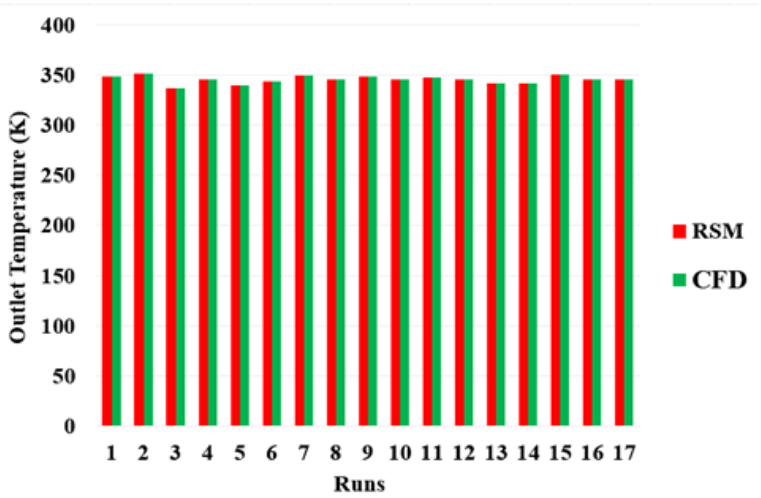

Fig. 3 Response factors for 17 runs

Figure 3 shows a bar graph comparing outlet temperature predictions from RSM and CFD simulations across 17 experimental runs. A run is associated with a specific set of parameters specified in the experimental design, including the secondary riser inclination angle, mass flow rate, and collector inclination angle. Interestingly, results from RSM and CFD processes show a high level of consistency across all runs, with insignificant differences between the 2 methods. This agreement confirms the RSM model's practical capability to predict the thermal efficiency of the solar flat plate collector system. Consequently, this combination of RSM and CFD simulation is shown as a stable and reliable method of enhancing solar thermal systems, which significantly helps in the design process and optimization procedures. STL (Stereolithographic) models of the solar collector system with various secondary riser inclinations of 10°, 45°, and 80° are presented in Figure 4. STL models represent the collector's geometry, highlighting structural differences or changes as the riser inclination is varied. CFD simulations rely on these models and enable systematic study of the effects of changes in riser inclination on fluid flow dynamics, heat transfer properties, and total thermal performance. By comparison of these few geometries, the study can find optimal riser inclination that enhances the efficiency of solar collectors, which provides the necessary knowledge for practical design and application of improved solar thermal systems.

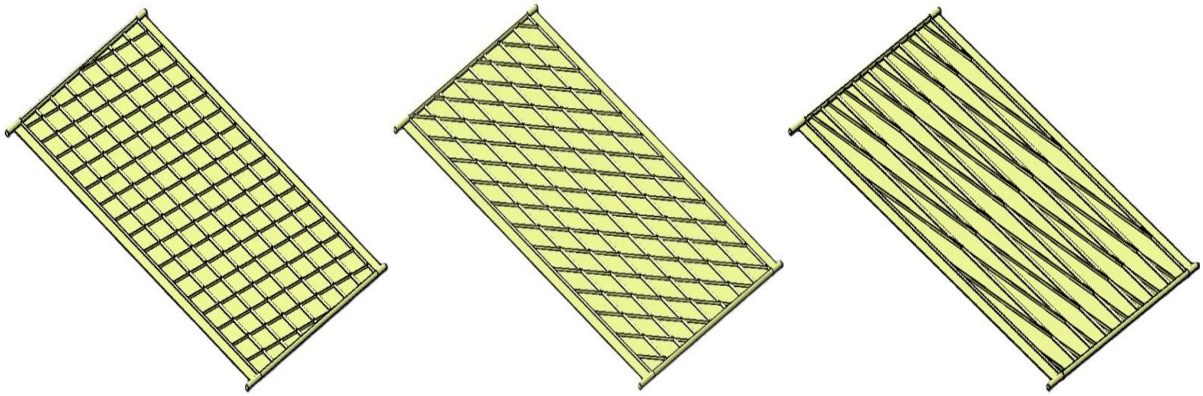

Fig. 4 STL model for secondary riser inclination at 10°, 45°, and 80°

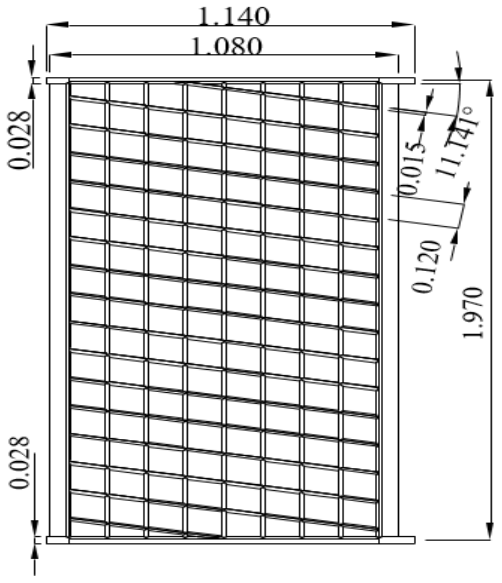

Fig. 5 Schematic diagram of the solar collector system with secondary riser inclination at 11.141° (all dimensions are in m)

Figure 5 represents a schematic representation of a solar collector system having a well-defined secondary riser inclination of 11.141°. The design clearly demonstrates important components, including the absorber plate, connecting riser pipes, and header pipes at the bottom and top. This figure of water flow path in the collector system highlights a proper heat transfer process through risers by indicating the entry and exit direction of water at the bottom header pipe and top, respectively.

5. Computational Fluid Dynamics

This study relied heavily on CFD to model and analyze the thermal and flow properties of the solar flat plate collector. To assess how key geometric and operating characteristics impacted the thermal performance of the system, a numerical model was developed to include secondary riser inclination angle, mass flow rate, and inclination angle. Using copper as absorber material and water as working fluid, the collector geometry was accurately modelled with real dimensions of absorber plate, header pipes, and risers. CFD simulations have been carried out in appropriate boundary conditions that include an input water temperature of 307 k and a mass flow rate of 23.628 kg/h with turbulence modelled in conventional parameters, including turbulent kinetic energy and dissipation rate. The field has been highly discretized, and a grid independence test was conducted to verify the accuracy of the solutions. To achieve steady convergence, solver parameters have been tuned for the energy, momentum, and turbulence equations. The simulations produced detailed insights into temperature distribution, heat transfer profiles, and outlet temperatures. The model outcomes have been confirmed contrary to experimental data and RSM predictions. CFD

model accurately predicted outlet temperatures with a deviation of only 0.167 K from the RSM-optimized value, demonstrating its reliability. Moreover, the CFD analysis helped visualize heat absorption dynamics across the absorber plate and riser tubes, confirming that a secondary riser inclination of 11.14° produced superior thermal performance. The results confirm the potential of CFD to accelerate solar thermal system development with improved predictive accuracy and reduced experimental overhead.

Fig. 6 CFD model for secondary riser inclination at 11.141°

The CED model of solar collector procedure is presented in Figure 6, where the secondary riser inclination angle is 11.141°. It is a numerical representation and simulation employed in this CFD model to study the temperature distribution in the collector system, fluid flow behaviour, and heat transfer efficiency. This model allows for accurately assessing and verifying optimal geometric parameters identified in the course of study and evaluating thermal performance comprehensively.

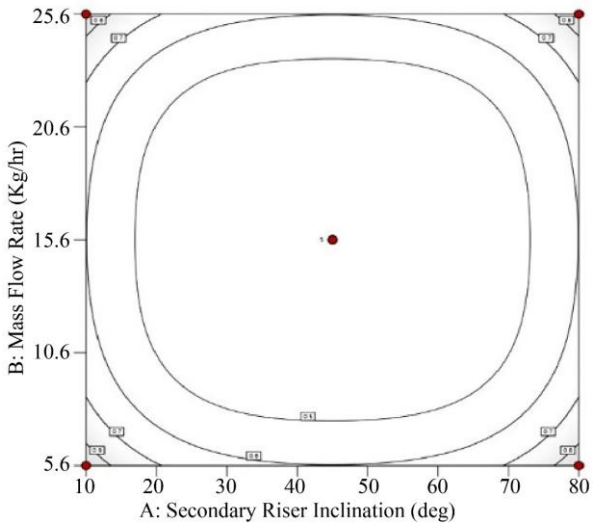

Fig. 7 3D plot for the effect of mass flow rate and angle of inclination on the outlet temperature

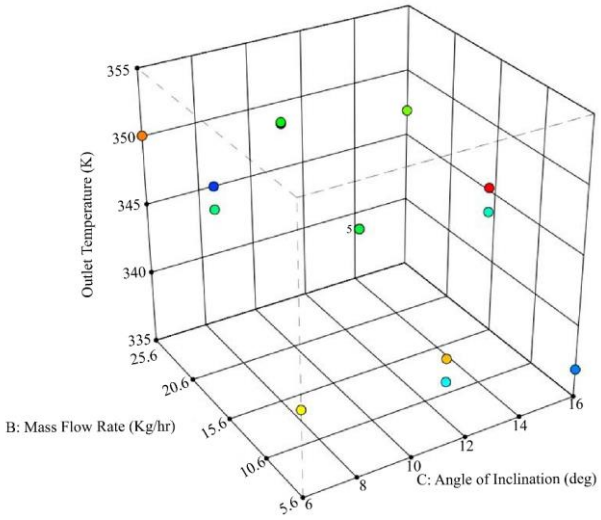

Fig. 8 Contour plot of standard error of design with secondary riser inclination and mass flow rate

A Three-Dimensional (3D) surface map showing the combined impact of collector inclination angle and mass flow rate on the solar flat plate collector's output temperature is shown in Figure 7. The graphic clearly shows that both factors have a significant impact on thermal performance. Outlet temperature first rises as the mass flow rate increases due to improved convective heat transfer; however, beyond an optimal point, further increases result in smaller temperature gains because there is insufficient dwell time for heat absorption. By altering solar insolation and the flow dynamics within the riser tubes, changes in the collector inclination angle also affect the outlet temperature.

A perfect tilt provides efficient fluid movement and maximizes sunlight capture. Figure 7 indicates that there is a specific point where 2 factors interrelate, with the highest outlet temperature occurring at an inclination angle of approximately 7.226° and an outlet mass flow rate of approximately 23.63 kg/h. These conditions give an optimum balance of flow rate, heat absorption, and gravity flow effects.

Figure 8 presents a contour plot of design standard error for 2 important design parameters: Secondary Riser Inclination and Mass Flow Rate. The contour lines in this two-dimensional figure reflect different degrees of standard error throughout the design space. Closely spaced contours or higher error zones indicate less accurate model predictions, while widely separated or lower-error regions suggest greater confidence and model accuracy. This image is handy for determining the most stable riser inclination and flow rate combinations for which the RSM model performs well. It also helps in making design decisions by steering clear of areas with high uncertainty, ensuring that solar collectors maintain consistent thermal efficiency. Figures 9 and 10 show the standard error distribution of the RSM-based regression model for the main design parameters of angle of inclination, mass

flow rate, and secondary riser inclination. A 3D surface map illustrating the standard error's variation with riser inclination and mass flow rate is depicted in Figure 9.

Model's dependability in those design ranges is confirmed by the flatter areas of the surface, which show zones of low prediction error, especially in the vicinity of the ideal values of 11.14° secondary riser inclination and 23.63 kg/h mass flow rate. This study is expanded into a cube plot in Figure 10, which shows the cumulative impact of all three components. The hue or height of the cube indicates the size of the standard error, and each corner corresponds to a particular parameter combination. It is important to note that the correctness and stability of the RSM model are verified by the lowest-error zone, which corresponds to the set of determined ideal parameters. Summation of the above numbers proves the accuracy of regression forecasts and gives confidence in selecting the optimal operating configuration to achieve better thermal performance.

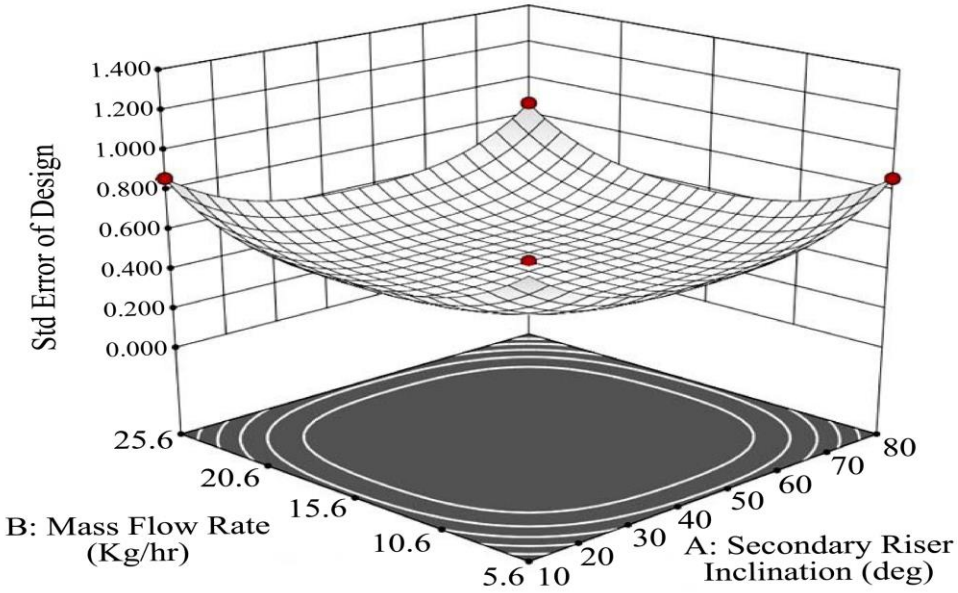

Fig. 9 3D surface plot of standard error of design as a function of secondary riser inclination and mass flow rate

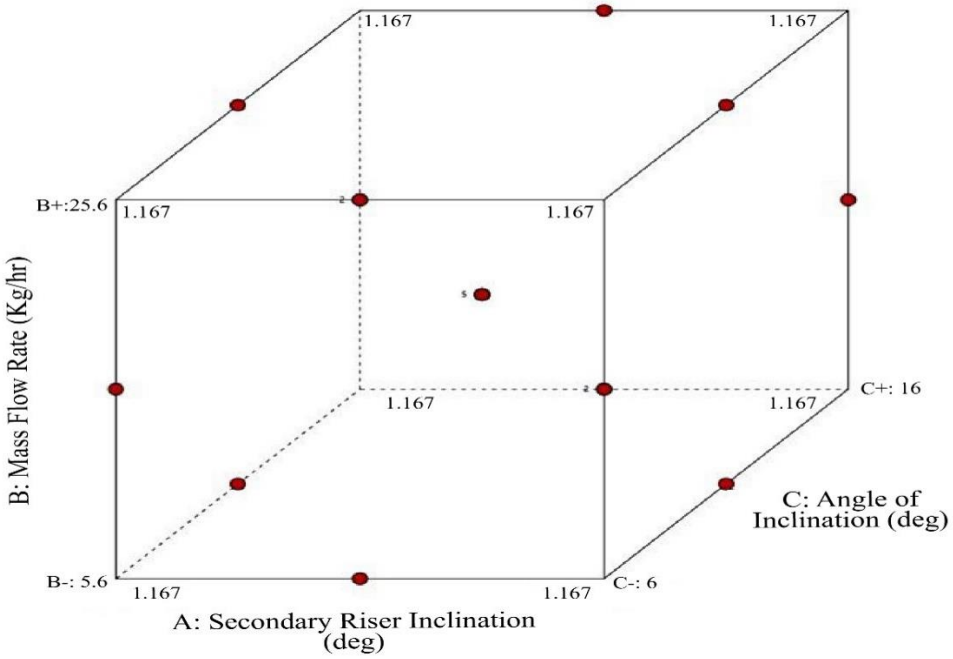

Fig. 10 Cube plot of standard error of design across secondary riser inclination, mass flow rate, and angle of inclination

Table 7. Analysis of Variance (ANOVA)

Source	Sum of squares	df	Mean square	*F*-value	*p*-value	
Mean vs Total	2.028E+06	1	2.028E+06	-	-	-
Linear vs Mean	204.09	3	68.03	24.12	< 0.0001	Suggested
2FI vs Linear	1.11	3	0.3709	0.1043	0.9557	-
Quadratic vs 2FI	29.58	3	9.86	11.55	0.0042	Suggested
Cubic vs Quadratic	5.98	3	1.99	-	-	Aliased
Residual	0.0000	4	0.0000	-	-	-
Total	2.028E+06	17	1.193E+05	-	-	-

Table 8. ANOVA for model significance

Source	Sum of squares	Df	Mean square	*F*-value	*p*-value	Significance
Model	234.78	9	26.09	30.56	< 0.0001	Significant
A-Secondary riser inclination	0.4051	1	0.4051	0.4746	0.5131	-
B-Mass flow rate	159.96	1	159.96	187.38	< 0.0001	Significant
C-Angle of inclination	43.73	1	43.73	51.23	0.0002	Significant
AB	0.7925	1	0.7925	0.9284	0.3674	-
AC	0.0162	1	0.0162	0.0189	0.8944	-
BC	0.3042	1	0.3042	0.3563	0.5694	-
A^2	8.11	1	8.11	9.50	0.0177	-
B^2	20.66	1	20.66	24.20	0.0017	Significant
C^2	2.36	1	2.36	2.77	0.1402	-

Table 9. Regression equation coefficients

Term	Coefficient
Intercept	+345.45
A (Secondary riser inclination)	-0.2250
B (Flow rate)	+4.47
C (Angle of inclination)	-2.34
AB (Interaction)	-0.4451
AC (Interaction)	-0.0636
BC (Interaction)	+0.2758
A^2 (Quadratic)	+1.39
B^2 (Quadratic)	-2.21
C^2 (Quadratic)	+0.7490

ANOVA (Analysis of Variance) was employed to evaluate various levels of the response surface model, including mean, linear, 2-Factor Interaction (2FI), Cubic, and Quadratic, as shown in Table 7. A table helps us to identify the model structure that best fits experimental data to estimate the outlet temperature. The linear model is very important ($p<0.0001$), showing a substantial impact of fundamental input parameters on response. Moreover, the quadratic model fits the 2FI model statistically ($p=0.0042$), which indicates inclusion of squared terms to explain curvature in the response. The cubic model is identified as being "aliased", meaning that it has fewer data points that can be correctly estimated. This analysis shows that the quadratic model is most appropriate to describe system behaviour and provide a balance between model correctness and complexity.

Tables 8 and 9 provide the statistics and math behind the regression model that improves how well a solar flat plate collector works. Table 8, along with ANOVA, indicates that the overall model is very important, with mass flow rate or angle of inclination being the significant parameters affecting exit temperature. Table 8, using ANOVA, indicates that the total model is very significant, with mass flow rate and angle of inclination appearing as the most relevant components impacting exit temperature. While secondary riser inclination has minimal individual relevance, its squared term adds significantly to the model's accuracy.

Table 9 shows the regression coefficients, demonstrating that mass flow rate has a significant positive influence on outlet temperature, whereas angle of inclination and riser inclination have negative trends. The inclusion of squared terms, especially for flow rate and riser inclination, shows that the system behaves in a nonlinear way as well as improves the model's capacity to make accurate predictions. These tables assure the RSM model's durability and accuracy in guiding performance optimization.

Figure 11 shows a Box–Cox plot showing the connection between the transformation parameter Lambda (λ) and the natural logarithm of residuals. This information helps determine the most effective data transformation for enhancing model accuracy. The green vertical line in this figure represents the ideal Lambda value, which is considerably different from 1, suggesting that the current dataset might benefit from a power transformation to stabilize variance and normalize residuals. The blue line at Lambda = 1 depicts the model without adjustment, indicating that utilizing raw data may not provide the most significant prediction results. Overall, the figure illustrates the requirement for an appropriate transformation to improve the dependability and statistical validity of the regression model.

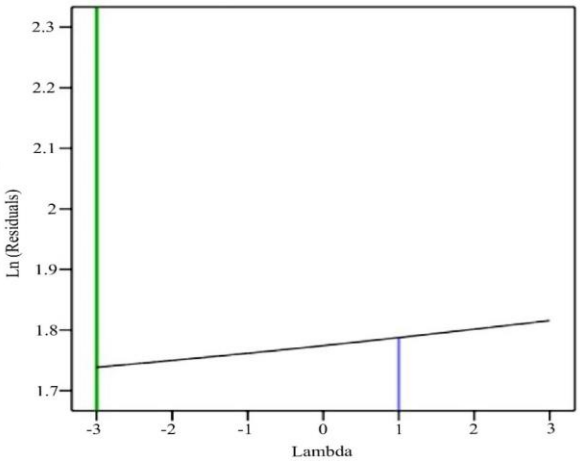

Fig. 11 Box–Cox plot of residuals for lambda transformation

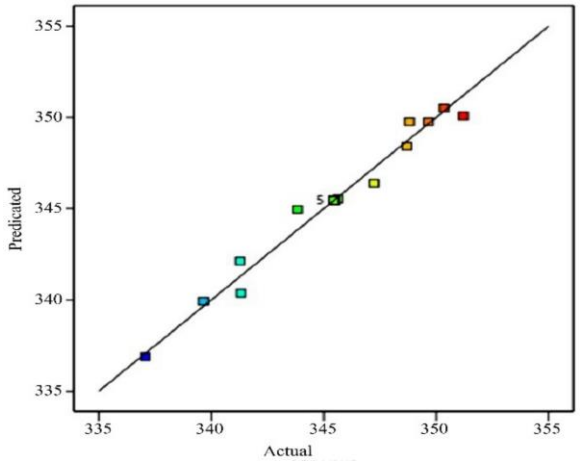

Fig. 12 Predicted vs Actual plot for model performance evaluation

Figure 12 shows the expected vs actual graph, which compares the accuracy of the regression model by comparing predicted outlet temperatures with actual experimental values. Every coloured point depicts one data run, and the solid diagonal line indicates a perfect scenario where projected values are equal to actual values. The proximity of data points with regard to this line means that there is a high correlation and high predictive accuracy of the model. Limited variations of line reveal limited residual errors and demonstrate that the RSM model reflects the relationship between design parameters and solar collector thermal performance well.

Figure 13 depicts a standard probability plot of external studentized residuals. The purpose of this Plot is to test whether residual of the regression model is normally distributed, which is a significant assumption for the model to be valid. Each point in this map represents a dataset residual, with the ideal normal distribution represented by the red diagonal line. The near alignment of most data points along a line implies that the residuals are generally roughly distributed, which lends credence to the model's statistical dependability and adequacy. Minor variations at the ends are permissible and anticipated, provided there are no severe outliers. Overall, this figure demonstrates that the model's residuals behave normally, which increases confidence in the model's predictions.

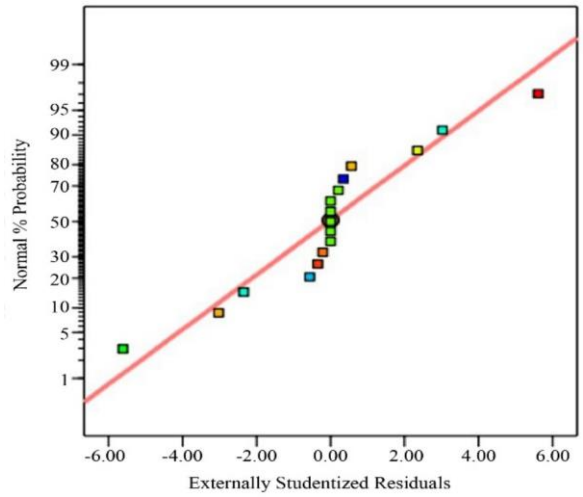

Fig. 13 Normal probability plot of externally studentized residuals

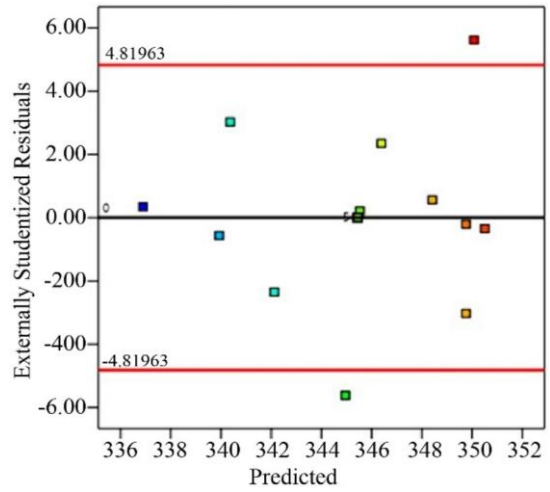

Fig. 14 Residuals vs Predicted values

Figure 14 shows a graph of externally studentized residuals vs predicted values. This graph is used to identify any outliers or trends that may indicate the model is not working correctly. Each point shows the regression model's error (or residual) for a predicted outlet temperature. Residuals should ideally be spread out randomly around the zero line, which would mean that mistakes are spread out and the model is not biased. The red lines on this map show the control limits, and most of the points are inside them (±4.81963). However, some points fall outside of these limits, which means that there are likely outliers or important observations. Nevertheless, the majority of residuals do not exceed acceptable limits, which means that the model is generally accurate and reliable, with some minor deviations that might require further investigation.

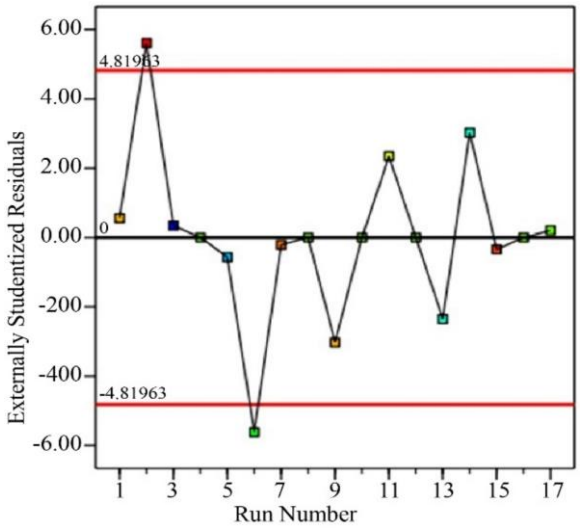

Fig. 15 Residuals vs Run order

Figure 15 depicts a plot of externally studentized residuals vs run number, which is used to identify probable outliers and look for systematic mistakes in the series of experimental runs. Each data point represents a particular run, and the residual indicates how much the model's forecast differed from the actual outcome for that run. The majority of points are around the horizontal zero line, suggesting a strong model fit. However, a few points fall outside the red threshold lines (±4.81963), identifying probable outliers or runs with a substantial effect on the model.

Despite these isolated deviations, the lack of a discernible trend or systematic pattern across run numbers indicates that the residuals are distributed randomly, supporting the premise of independence and validating the model's consistency across all experiments. Figures 16 and 17 show two essential diagnostic plots: Cook's distance vs run number and leverage vs run number, which are used to analyze the effect of individual data points on the regression model. The Cook's distance figure indicates that most runs are below the 1.0 threshold line, suggesting they have little impact on the model. However, a few points, notably runs 1, 4, and 6, surpass this threshold, indicating that these runs have a significant effect and may disproportionately alter the regression findings. The leverage plot confirms this finding by showing leverage values above the cut-off (about 0.588), suggesting that these runs are at the extremes of the design space and have a significant effect on the fitted values. These plots assist in highlighting important and high-leverage observations that need more investigation to verify the model's robustness and reliability.

Figures 18 and 19 illustrate influential diagnostics that evaluate the efficacy and stability of regression models based on individual data points. The DFFITS (Difference in Fits) graphic in Figure 18 shows how much the predicted value for a specific observation changes when that data is left out of the regression model. Data points that are higher than the control threshold (±2.30089) are very important since removing them will change the model's anticipated output in a big way. Several runs in this Plot go above the threshold, which means that there are points that affect the model that are too big and should be looked at more closely.

The DFBETAS (Difference in Beta Estimates) plot for the intercept coefficient is shown in Figure 19. It shows how each observation changes the estimate of the regression intercept. All of the data points are still well within safe range (±0.727607), which shows that no one observation has too much of an effect on the model's intercept term. All of these numbers demonstrate that the fundamental regression structure, especially the intercept term, is statistically stable, even when specific data have a significant impact on anticipated outlet temperature (as revealed by DFFITS). This in-depth study reinforces that the RSM model that was built is reliable and strong.

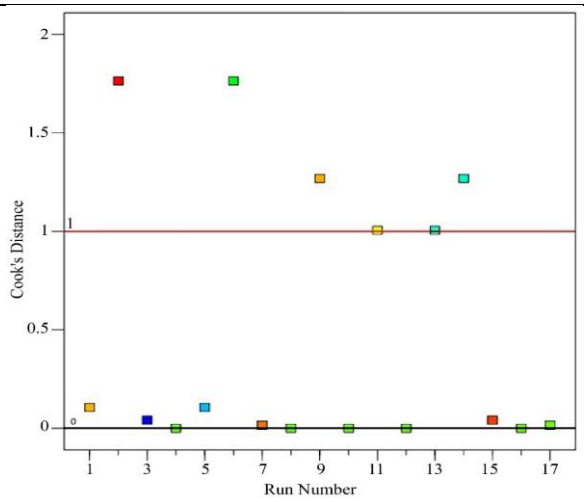

Fig. 16 Cook's distance plot

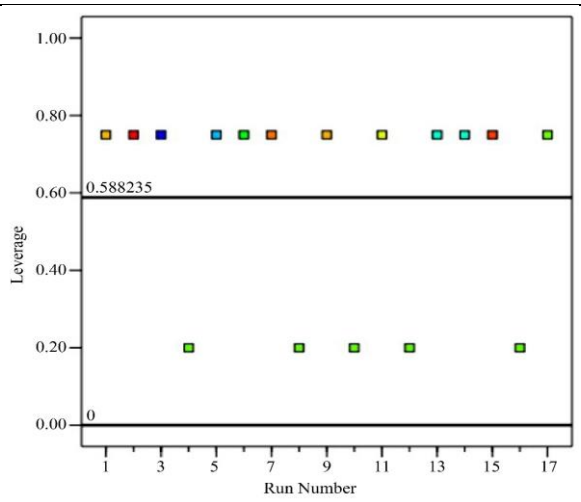

Fig. 17 Leverage plot

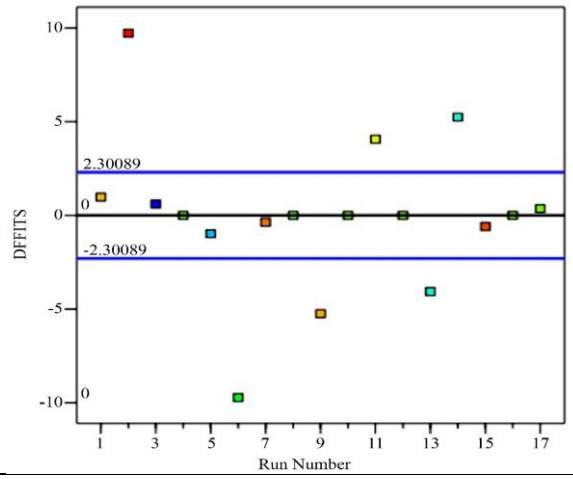

Fig. 18 DFFITS vs Run

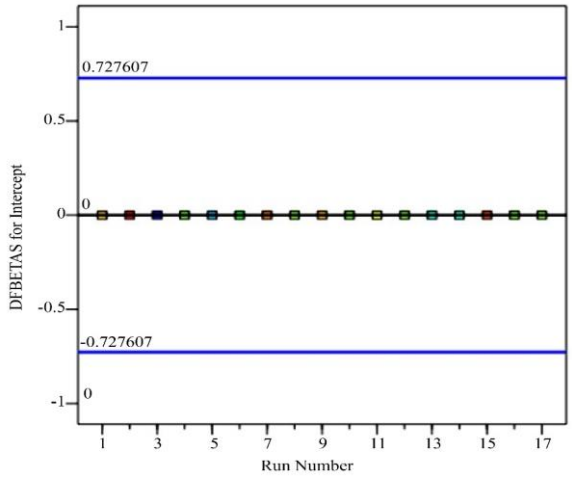

Fig. 19 DFBETAS for intercept vs Run

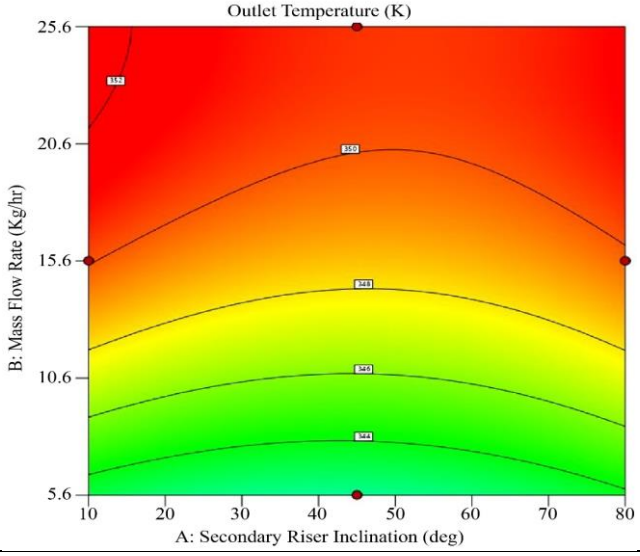

(a)

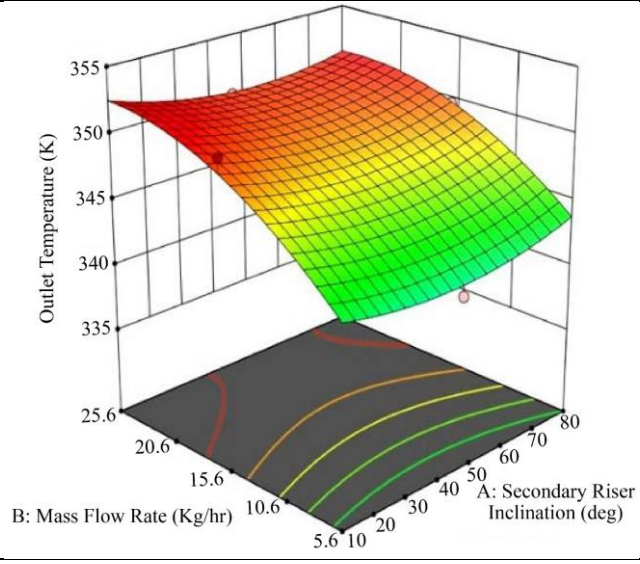

(b)

Fig. 20 Effect of outlet temperature vs. Secondary riser inclination and mass flow rate: (a) Contour plots, and (b) 3D surface plot for angle of inclination in 6°.

The influence of mass flow rate and secondary riser inclination on outlet temperature at three distinct inclination angles, 6°, 11°, and 16°, respectively, is shown in Figures 20, 21, and 22.

Each graphic displays both 3D surface plots and contour plots. For various parameter combinations, contour plots provide constant outlet temperature zones, and the 3D plots clearly illustrate how temperature varies depending on the two factors.

The surface is smoother, and the temperature change is less sharp in Figure 20, which shows a modest reaction at an inclination angle of 6°. The temperature rises more quickly at an 11° inclination in Figure 21, indicating that this angle facilitates heat transmission more effectively. The relationship between secondary riser angle and flow rate is evidently greater. For a 16° slope, Figure 22 shows a steeper surface and a rapid shift in output temperature with parameters. This graph demonstrates that when the inclination angle increases, the system's sensitivity increases. With a smoother stability and a greater output temperature, the 11° tilt (Figure 21) offers the finest performance balance of all.

These figures indicate which combinations of parameters provide the best thermal performance and validate that the tilt angle of the collector must be used for optimizing the secondary riser's inclination and flow rate. Combined use of CFD simulation and RSM provided a reliable framework to determine and optimize the thermal performance of a solar flat plate collector. Current methodology ensured accurate prediction, minimized experimental effort, and identified the optimal parameter settings for maximum efficiency.

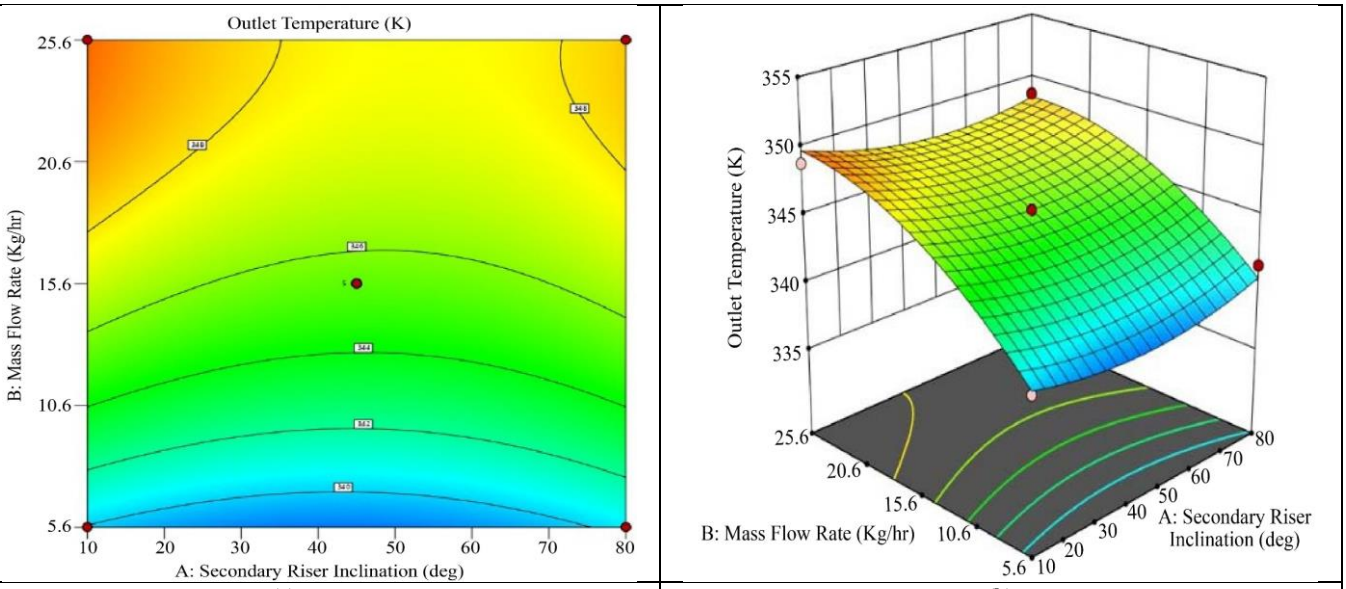

(a) **(b)**

Fig. 21 Effect of outlet temperature vs Secondary riser inclination and mass flow rate: (a) Contour plots, (b) 3D Surface plot for angle of inclination at 11°.

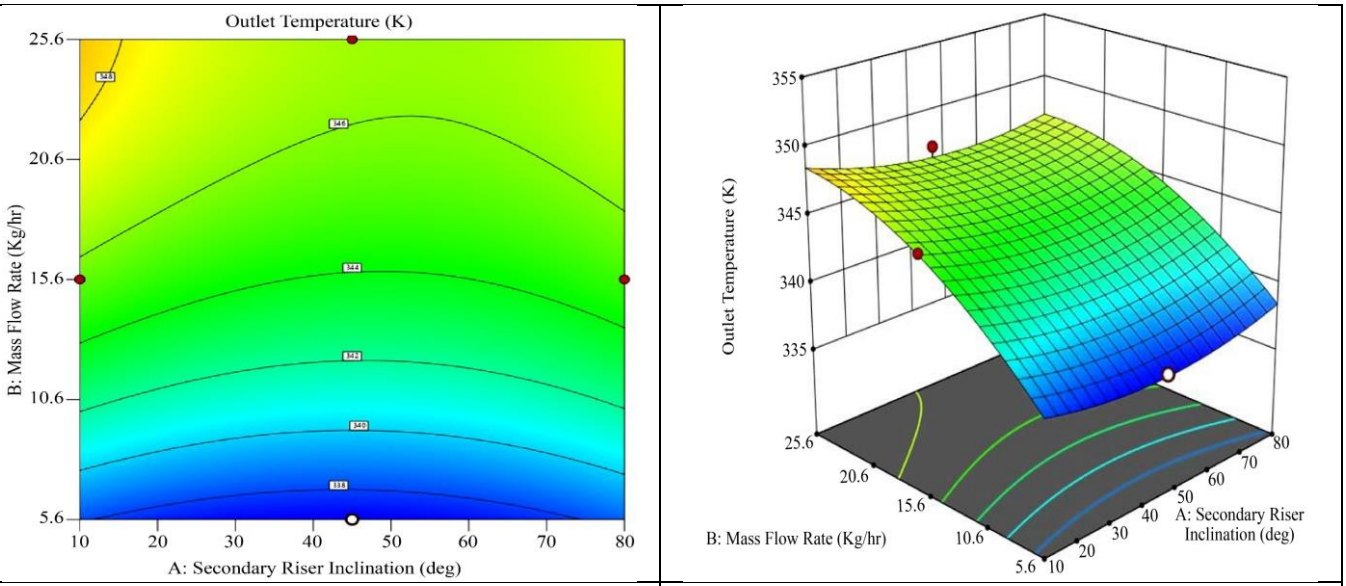

(a) **(b)**

Fig. 22 Effect of outlet temperature vs Secondary riser inclination and mass flow rate: (a) Contour plots, (b) 3d surface plot for angle of inclination at 16°.

5.1. Uncertainty Analysis

The current methodology is doubtful due to the geometric specifications, operation conditions, numerical modeling, and statistical regression involved in the coupled RSM-CFD framework. The uncertainty of hydraulic diameter, area of heat transfer, and distribution of flow owing to fabrication and measurement tolerances with pipe spots, the thickness of the absorber plates, and space between the risers directly impacts the predictions of convective heat transfer. There are operational uncertainties with the inlet temperature, mass flow rate, and the collector and secondary riser inclination angles, which impact the residence time, buoyancy effects, and thermal gradients in the collector. In the CFD simulations, there is another source of uncertainty in the definition of boundary conditions, prescribed values of turbulence, mesh discretization, and convergence criteria of the solver. Despite the use of grid independence tests and high tolerances of residual, numerical residual, and turbulence model-form uncertainties, they are still inevitable despite a large number of studies that have reported CFD-based heat transfer (Oberkampf and Roy, 2010).

The Response Surface Methodology is associated with statistical uncertainty, in which the effectiveness of the surrogate models is based upon how many times the experiment is run and whether the quadratic regression is sufficient to capture the nonlinear interactions. The Box-Behnken design is effective at capturing both main and interaction effects as the design space is defined. However, predictive uncertainties are larger than this range, as observed in the literature of surrogate modeling (Forrester et al., 2008). The significant coefficient of determination (R2 = 0.9994) in this research implies that there will be minimal unexplained variance, but still, there will be inherent regression and experimental noise that will add up to overall uncertainty. An intense match between the CFD and RSM predictions, as indicated by the most significant outlet temperature difference of 0.167 K, indicates that the cumulative propagated uncertainty is not excessive and does not exceed the engineering tolerability. The degree of such uncertainty is the same as that of recent coupled CFD-RSM investigations and proves the strength and validity of the methodology chosen to optimally characterize the performance of the solar flat plate collector.

6. Results and Discussions

In this section, RSM and CFD are used to simulate and optimize a solar flat-plate water-heating system. The results provide valuable new insights into the performance gains achieved through optimization of design parameters. The findings are discussed in depth in the following sections.

6.1. Optimization with Desirability Function Analysis

The ramp function in Figure 23 shows how the optimization process works by illustrating how desirable each parameter, secondary riser inclination, mass flow rate, and angle of inclination, is for achieving the target outlet temperature of 351.448 K, which has a perfect desirability score of 1.000. The optimal values for secondary riser inclination (11.141°), mass flow rate (23.6277 kg/h), and angle of inclination (7.22633°) are consistent with the system's performance objectives. The graph demonstrates the considerable impact of mass flow rate and riser tilt on thermal efficiency, with values at the top range ensuring maximum heat transfer. This tool efficiently displays factor interactions, offering valuable insights for developing high-performance Solar Collector Systems.

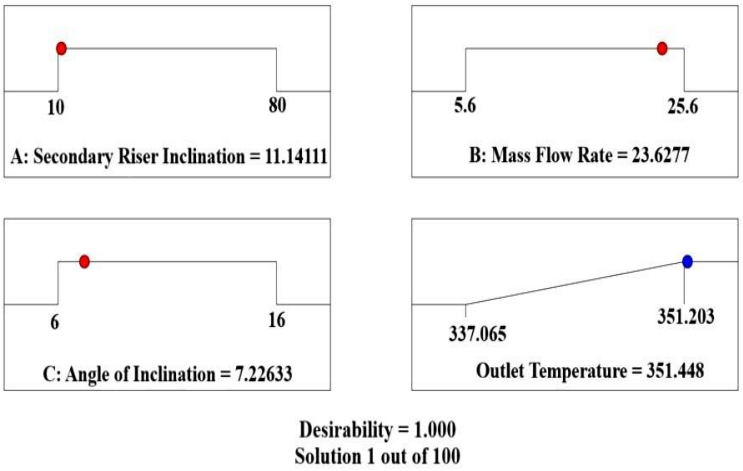

Fig. 23 Ramp function graph of desirability for optimization parameters

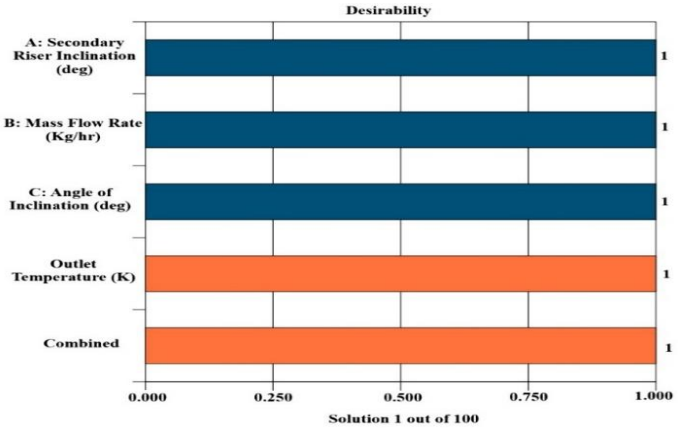

Fig. 24 Desirability bar chart for optimization parameters

Figure 24 shows a bar chart that illustrates the best results for solar flat plate collector design utilizing RSM for various working parameters. Each horizontal bar represents a design factor, like secondary riser inclination (A), Mass Flow Rate (B), and Angle of Inclination (C), along with the response variable (outlet temperature) and overall desirability. Each horizontal bar shows a design variable, such as Secondary Riser Inclination (A), Mass Flow Rate (B), Angle of Inclination (C), as well as the response variable (outlet temperature) and combined desirability. All parameters have a maximum desirability value of 1.0, indicating that the chosen parameter combination produces optimal optimization outcomes for all input and output criteria. This means that the solution not only meets but fully achieves the goals of increasing outlet temperature while keeping the best design conditions, proving that the model is good at finding the best operating settings for better thermal performance.

6.2. Analysis of Contour and Surface Plots

In Figure 25 (a), the contour plot shows the link between Secondary Riser Inclination (A) and Mass Flow Rate (B) in establishing the suitability of the solar flat plate collector's performance. The gradient between the desirability of green (lower desirability) and red (greater desirability) determines the optimal point at which the system will achieve an ideal desirability score of 1.000. The optimal riser inclination reading is 11.14°, and the rate of mass flow is 23.63 kg/h. Circles in the figure represent places with fixed desirability, which show how optimising these parameters leads to better system efficiency. The figure shows that the equilibrium between riser inclination and mass flow rate is significant in attaining optimal thermal efficiency and outlet temperature of the system. Figure 25 (b) depicts the relationship between Secondary Riser Inclination (A) and Mass Flow Rate (B) in the context of system thermal performance in a 3D surface map. The surface moves between green (low desirability) and red (high desirability), indicating that the optimal combination of parameters leads to the highest desirability score of 1.000. The slope of the surface would illustrate the degree to which the performance of the system varies with these parameters, because an increase in riser angle to a point of about 11.14° and an increase in mass flow rate to 23.63 kg/h would go a long way in improving the thermal efficiency of the system. Gradient and curvature of the surface underline nonlinear interaction between parameters, emphasising the necessity to find a perfect balance to increase attractiveness and reach the highest possible performance of the system. This diagram shows the effectiveness of adjusting different design parameters to enhance thermal efficiency.

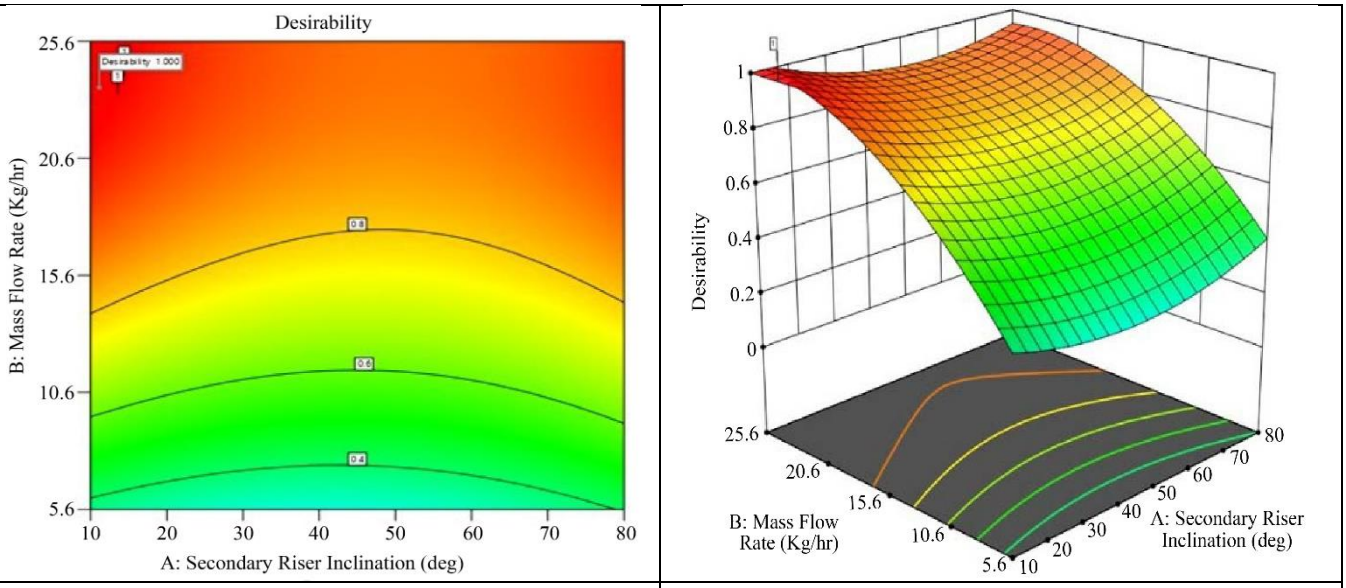

(a) **(b)**

Fig. 25 Effect of desirability vs Secondary riser inclination and mass flow rate: (a) Contour plots, and (b) 3D surface plot.

Figure 26 (a) presents a contour map of the influence of secondary riser tilt (A) and mass flow rate (B) on the output temperature of the solar flat plate collector system.

Colour gradient is green (low outlet temperature) to red (high outlet temperature), where the highest temperature is 351.448 K at optimum riser inclination of 11.14° and mass flow rate of 23.63 kg/h. Circular shape lines reflect the temperature of the outlet at all times, which requires parameter adjustment. The graphic demonstrates that a high rate of mass flow enhances the efficiency of heat transfer to a given limit, but proper riser tilt enhances turbulence and heat absorption. These results illustrate that precise changes in parameters are required to achieve maximum thermal efficiency with solar collector systems.

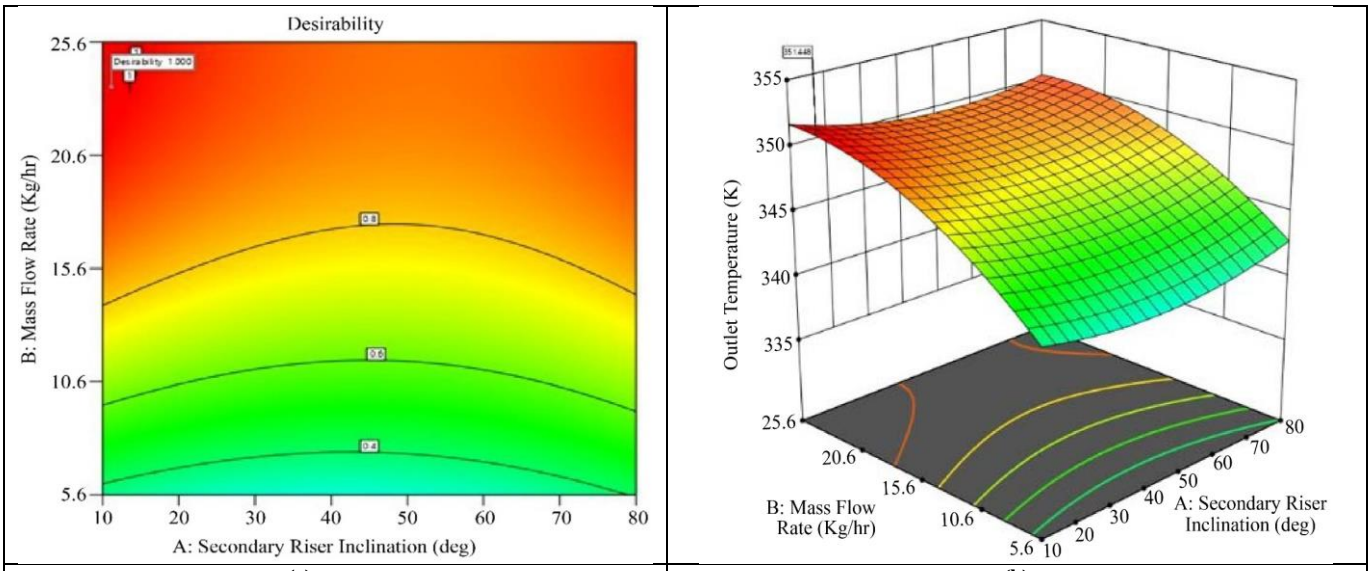

(a) (b)

Fig. 26 Effect of outlet temperature vs Secondary riser inclination and mass flow rate: (a) Contour plots, and (b) 3D surface plot.

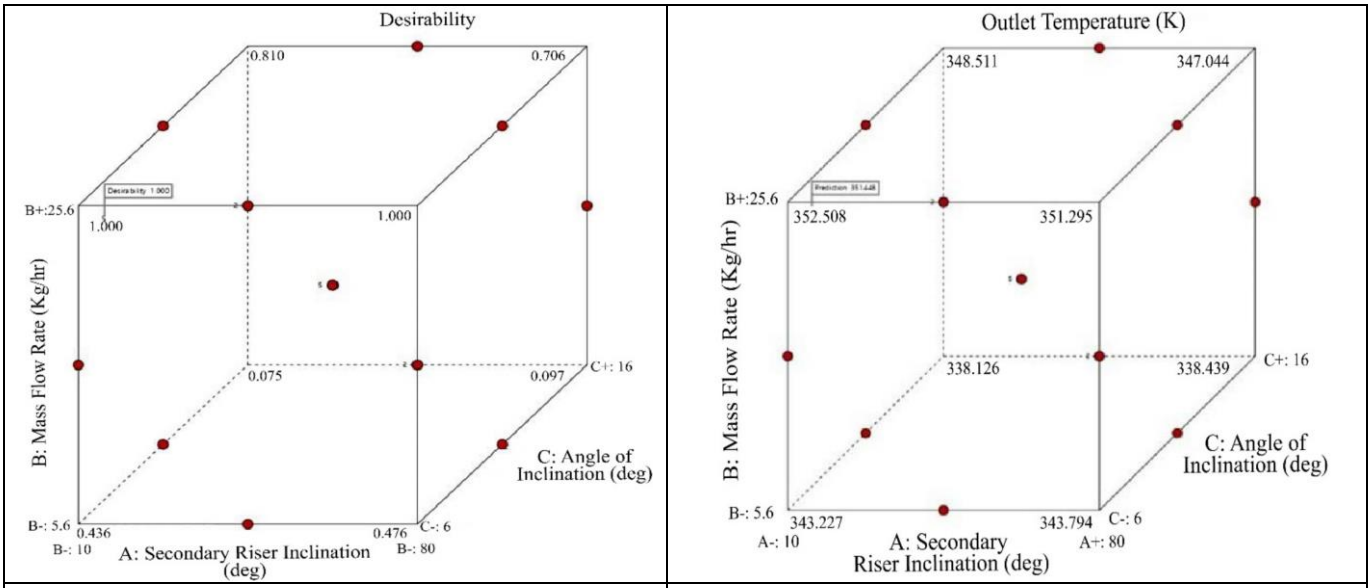

(a) (b)

Fig. 27 Cube of: (a) Desirability, and (b) Outlet temperature across parameters.

In Figure 26 (b), the 3D surface illustrates the impact of Secondary Riser Inclination (A), Mass Flow Rate (B) on the outlet temperature of the solar flat plate collector system. The surface changes to red (higher temperatures) from green (lower temperatures), proving that the optimal outlet temperature of 351.448 K is achieved at an 11.14° riser inclination and mass flow rate of 23.63 kg/h. Sudden shift on the surface reflects the extent to which both variables are crucial, riser inclination enhancing turbulence to facilitate improved heat transfer and mass flow rate, balancing fluid flow to improve energy absorption. Parameters become non-ideal, and the surface flattens, which means that thermal performance is not good. This figure demonstrates the significance of parameter tuning in attaining maximum thermal efficiency and boosting system performance. Figure 27 presents cube graphs demonstrating the influence of Secondary Riser Inclination (A), Mass Flow Rate (B), and Angle of Inclination (C) on the attractiveness or outlet temperature of a solar flat plate system in heating water. A combination of parameters, as defined as ideal: secondary riser inclination of 11.14°, mass flow rate of 23.63 kg/h, angle of inclination of 7.23°, is most desirable with a score of 1.000 in the desirability cube, which depicts efficiency of parameter manipulation. Cube of outlet temperature indicates that the estimated ideal outlet temperature of the same parameter values is 351.448 K, and this shows the synergetic effect of these parameters on thermal efficiency. Both figures explicitly display the influence of changes in any of the 3 parameters on

the performance of the system, which is why it is important to balance them to achieve the most successful results. Visualisations are practical in planning and enhancing solar thermal systems to ensure maximum energy efficiency.

6.3. Perturbation Analysis

Graphs in Figure 28 depict how variations in 3 key input variables, including Secondary Riser Inclination (A), Mass Flow Rate (B), and Angle Of Inclination (C), influence the performance of the system, quantified by desirability and outlet temperature. Graphs indicate that Mass Flow Rate (B) is most sensitive to attraction and output temperature, as indicated by a sharp curve. The figure highlights the importance of enhancing fluid flow dynamics and heat transfer efficiency.

Mass flow rate is very effective in enhancing performance up to the optimum level, but further increases are not very effective. This is significantly influenced by the secondary riser inclination (A), resulting in a different, but not as steep, performance curve. This parameter enhances turbulence and heat transfer, thereby improving the system's performance. Angle of Inclination (C) has little effect, as shown by the flat curve, indicating that variations in this parameter do not significantly affect the system's thermal efficiency or attractiveness. Generally, graphs emphasise the need to work on optimization of mass flow rate and inclination of secondary risers to improve the performance of the system, but also leave the opportunity to adjust the angle of inclination in actual use.

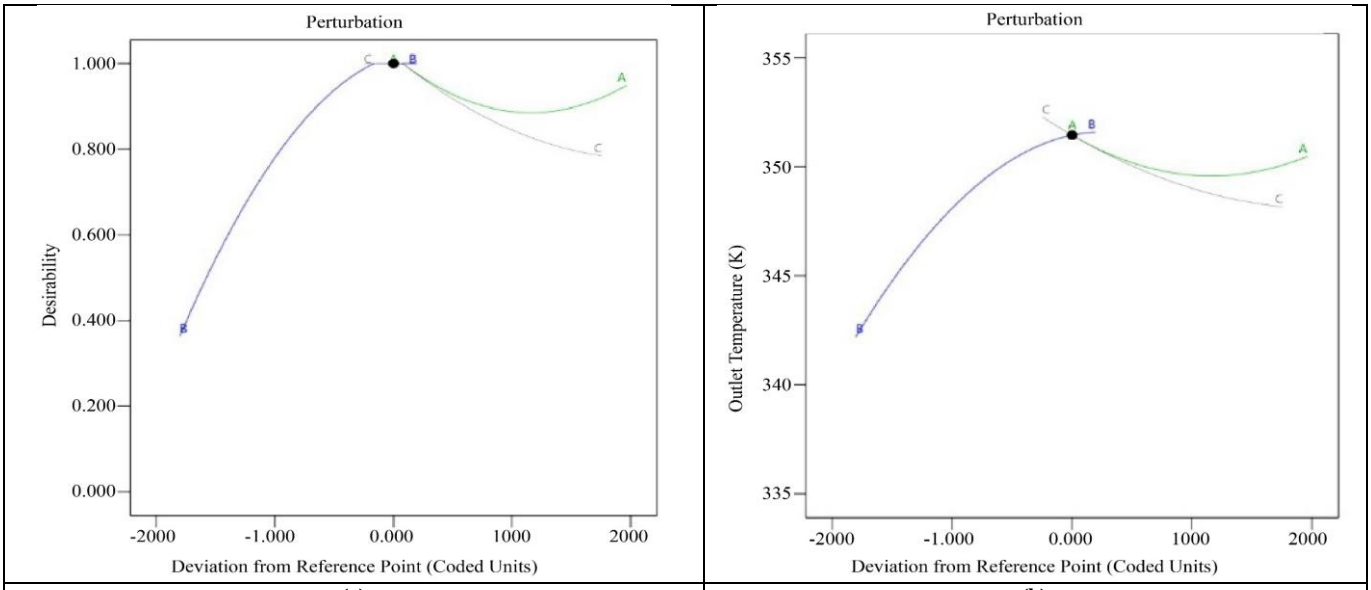

(a) **(b)**

Fig. 28 Perturbation Analysis of: (a) Desirability, and (b) Outlet Temperature,

6.4. Temperature Distribution Contour in the Solar Flat Plate Collector's Absorber Plate

Figure 29 shows the temperature distribution contour of the solar flat plate collector and indicates the thermal gradient between the input and output. The illustration shows fluid flowing into the collector at low temperature and slowly gaining heat in passing through the riser tubes and through the absorber plate. We see a huge temperature rise, which indicates effective movement of heat between the surface that is being heated by the sun and the working fluid. All higher temperatures are concentrated around the exit, and this implies that most of the thermal energy has been absorbed before the fluid moves out of the collector. This distribution illustrates the efficiency of the collector to transform solar light into useful thermal energy, as well as verifying the design and material structure under simulated conditions. The CFD running model has variable runs of 1200s, 2400s, 3600s, 4800s, 6000s, 7200s, 8400s, 9600s, 10800s, 12,000s. When compared with other running models, the outcomes from 12,000s are superior.

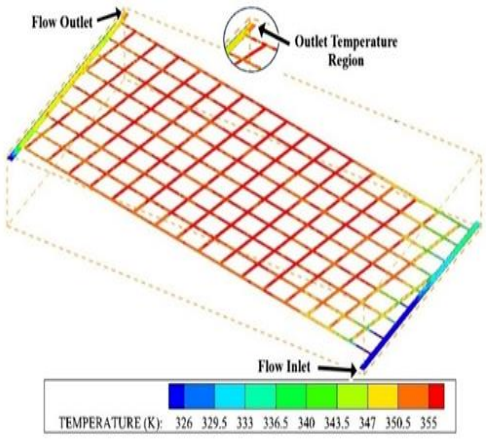

Fig. 29 12,000 s Running Model for CFD

6.5. Comparison between the RSM and CFD

Figure 30 displays the output temperature of the solar flat plate collector estimated utilizing two techniques, viz, RSM and CFD. The red bar indicates the output temperature received via RSM, whereas the green bar depicts the temperature projected by CFD. Both techniques provide almost identical answers with just a slight variance, demonstrating excellent agreement and model validation. This strong link confirms that the RSM model accurately predicts how well the system performs in terms of heat, making it a valuable tool for optimization when experiments or CFD analysis are expensive to run.

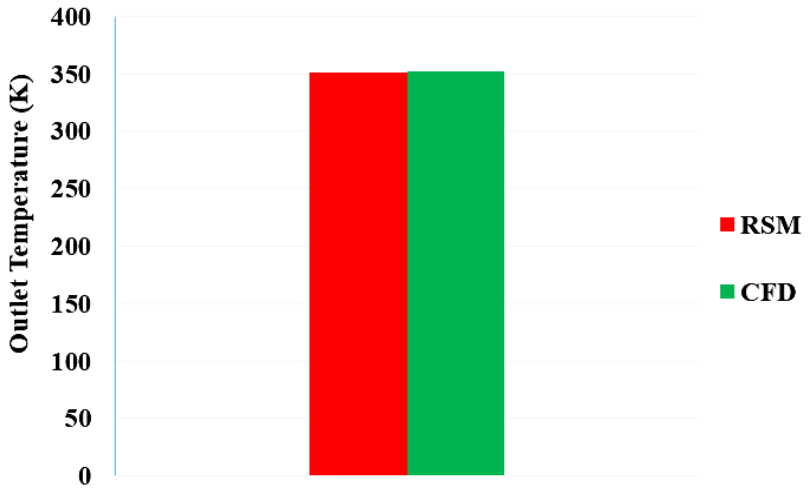

Fig. 30 Validation of outlet temperature RSM and CFD optimal model

6.6. Comparison of Results and Methods with Recent Studies

The results of the current research in performance are comparable to the recent industrial standards and scientifically published models in the optimization of solar flat plate collectors. The current literature suggests that traditional geometric and operational optimization methods can generally improve thermal efficiency by 18-35% once, and more advanced optimization methods can claim efficiencies of up to 80-86% when using nanofluids or flow improvement methods under controlled numerical or laboratory conditions (Desisa et al., 2023). Optimal tilt angles of 7° through 15° and mass flow rates of 20-30 kg/h are common in industry-oriented experimental and numerical research on realistic operating conditions, yet give peak outlet temperatures and thermal efficiencies of 60-65 percent with standard water-based flat plate collectors (Alsadi & Foqha, 2023). In this framework, the optimum parameters of the current study, such as mass flow rate of 23.628 kg/h, secondary riser inclination of 11.141°, and collector inclination of 7.226°, are well within industrial design envelope parameters, and the outlet temperature is high (351.448 K).

The integrated CFD-RSM framework used here has better predictive power compared to the existing models, as seen by the fact that the difference between the numerical and statistical predictions (0.167 K) is negligible and the regression prediction power (R2 = 0.9994) is exceptionally good. In contrast to most industrial design methodologies, which make extensive use of an iterative experimental process or optimization of a single parameter, the current method achieves similar or better thermal performance with a lower experimental cost. The findings also suggest that mass flow rate and inclination angle are prevailing factors influencing thermal efficiency, which supports the already existing findings on effects of flow dynamics and geometric orientation in solar collectors (Omo-Oghogho & Aliu, 2020; Qader et al., 2018). The nonlinear system behavior reproduced by quadratic regression models underscores the presence of nonlinear parameter interactions, as observed in CFD-RSM-based studies (Kazemian et al., 2024; Kola et al., 2021). The most optimal secondary riser inclination of about 11.14° supports the fact that design optimization can be effective even with a primary goal of improving the heat transfer by geometric refinement, as previously reported in the literature in the design optimization efforts (Thejaraju et al., 2017). The choice of copper as the absorber material and water as the working fluid aligns with the traditional practice in flat-plate collectors (Vengadesan & Senthil, 2020). Although recent literature has focused on nanofluids and novel materials to enhance performance (Vyas et al., 2024; Desisa, 2023), this study provides a supportive and economical optimization pathway that acts on geometric and flow parameters and supports the use of CFD-RSM integration as a scalable and accurate optimization tool in solar flat plate collector optimization (Toffolo, 2008).

6.7. Environmental Impacts and Life Cycle Considerations

The Environmental Impact Analysis of the optimized solar flat plate collector developed under this research gives a requisite contribution to the thermal performance enhancement brought by the joint implementation of Response Surface Methodology and Computational Fluid

Dynamics. An in-depth sustainability assessment should be conducted, including Life Cycle Assessment and embodied carbon analysis to assess environmental impacts across all processes, such as the extraction of raw materials, component production, transportation, operation, and product disposal. In this context, the fact that copper is used as the absorber material, although beneficial because of its high thermal conductivity, presents significant embodied energy and carbon costs related to the mining and processing of copper. The design parameters, geometrically determined by the methodology (e.g., absorber plate thickness, riser pipe dimensions, etc.), affect material consumption and, therefore, reflect environmental impacts. The optimization outcomes that illustrate enhanced thermal performance under specific riser inclination and flow conditions imply that greater energy recovery during operation can compensate for these embodied influences on the system's service life.

The importance of material efficiency and thermal performance balance is also emphasized by the concept of embodied carbon. To produce greenhouse gas, the copper absorber plate and piping contribute most of the greenhouse gas emissions of a system's production, and thus, an optimized design is needed to reduce the amount of embodied carbon per unit of sound thermal energy provided. The optimized and CFD-validated operations with the operating parameters of the mass flow rate of 23.628 kg/h and the secondary riser inclination of 11.141° provide a greater outlet temperature of 351.448 K and, hence, a better overall system efficiency and the minimization of reliance on auxiliary energy sources. The CFD-RSM framework can, in conjunction, be used to integrate the performance and environment measures since it is able to allow material-efficient geometries without affecting thermal output. The next generation of work should involve high LCA modelling using the optimal parameters found in this paper to measure the trade-off between the embodied and operational emissions and to investigate other low-embodied-carbon materials or new heat transfer fluids to enable further improvement of sustainability. Together, the current methodology creates a strong framework for the design of a solar flat plate collector that is environmentally aware, such that any increase in thermal efficiency results in real lifecycle environmental performance.

6.8 Extended Case Study or Validation

The study should be expanded to provide more long-term research on the current CFD-RSM framework to increase its strength, usability, and practicality in a wide range of operating conditions. By introducing several climatic conditions (tropical, temperate, and arid), it would be possible to test the stability of the model across different solar insulations, ambient temperature, and humidity conditions. The use of alternative fluids like nanofluids and phase change materials, among others, in addition to the already used ones, would make it even more straightforward to determine how they affect thermal efficiency and predictability, especially in the context of industrial-scale applications. To improve model adaptability, it is possible to investigate a wider variety of geometric configurations, such as other riser arrangements and alternative plate thicknesses of absorbers (not limited by the current set of limits), along with alternative construction materials. The combination of long-term transient CFD simulations and real-world operation data, representing the diurnal and seasonal variations, would enhance long-term predictability compared to the present transient analysis period. Simultaneously, it needs to be validated experimentally in several prototype configurations and operating regimes, in order to be generally applicable. However, lastly, the use of multi-objective optimization, which would also consider thermal performance in addition to pressure drop, economical cost, and environmental impact, with a larger or alternative design-of-experiments framework than the Box-Behnken method, would be beneficial in terms of statistical power and would offer a more complete foundation to constructive solar flat plate collector design. These expansions will increase the generality of the model to include a broader range of conditions and allow it to be used in a wide range of designs of solar thermal systems.

7. Conclusion

During this research, optimization and simulation have been performed on a solar flat plate collector system utilizing a combined procedure of CFD and RSM. Combining both approaches, we have created accurate models that prevail in enhancing the thermal performance of the system, making them more accurate and predictable. The 3 main factors considered were Mass Flow Rate (kg/h), Secondary Riser Inclination (Degrees), and Angle Of Inclination (Degrees). In RSM, 17 experimental runs have been evaluated utilizing the Box-Behnken design. The regression model exhibited excellent predictive capacity (R2=0.9994, adjusted R2=0.9985, and predicted R2=0.9958) and indicated a high level of correspondence between expected and actual values.

The model estimated the highest outlet temperature of 351.448 K with a desirability score of 1.000. optimal combination has been observed at a mass flow rate of 23.628 kg/h, secondary riser inclination of 11.141°, and angle of inclination of 7.226°. A CFD simulation was used to verify this optimal condition. CFD-calculated outlet temperature (351.615 K) was within 0.167 K of the RSM value, indicating the accuracy and reliability of the model. In ideal conditions, CFD exhibited a mean collector temperature of 340.89 K and a mean absorber plate temperature of 339.42 K. Transient thermal analysis in CFD, over a total simulation length of 12,000s, showed an overall steady, progressive rise in temperature, leading to a very close match with the RSM prediction. Plots and velocity contours were streamlined to ensure that the flow was correctly distributed in headers and risers. Pressure drop and turbulence intensity were also checked to ensure that the system remains hydraulically efficient. The temperature of output calculated by RSM

(351.448 K) and CFD (351.615 K) varied by only 0.167 K, which meant that both methods were relatively accurate.

This confirmation demonstrates that RSM can be considered as a credible option to advance the system, decreasing the amount of calculation to perform extensive simulations.

Temperature maps by CFD indicate constant heat uptake and satisfactory distribution of flow over the collector that supports thermodynamic design and corroborates optimization findings. The findings indicate that CFD and RSM are harnessing tools that are reliable, scalable, and low-cost to optimise solar thermal systems. The method is not only fast in the design process but also reduces reliance on time-consuming trial-and-error experiments. Moreover, the established model offers a feasible guideline in upcoming research in transient analysis, climate-indirect evaluation, and application of advanced heat transfer fluids, such as nanofluids and phase change materials.

The study contributes immensely to the literature on renewable thermal systems as it offers a replicable model that can be applied to different solar energy systems. The next step in research may involve real-world testing and checking of costs and benefits with an aim of increasing the use of improved solar thermal technology.

Data Access Statement

The data that support the findings of a study are available from the corresponding author upon reasonable request

References

[1] Moslem Abrofarakh, and Hamid Moghadam, "Enhancing Thermal Performance and Reducing Entropy Generation Rate in Evacuated Tube Solar Air Heaters with Inserted Baffle Plate using Static Mixers: A CFD-RSM Analysis," *Thermal Science and Engineering Progress*, vol. 55, 2024. [CrossRef] [Google Scholar] [Publisher Link]

[2] Anil Singh Yadav, and Jiwanlal Bhagoria, "Heat Transfer and Fluid Flow Analysis of Solar Air Heater: A Review of CFD Approach," *Renewable and Sustainable Energy Reviews*, vol. 23, pp. 60-79, 2013. [CrossRef] [Google Scholar] [Publisher Link]

[3] Lotfi Ben Said et al., "Application of Box-Behnken Design with RSM to Predict the Heat Transfer Performance of Thermo-Magnetic Convection of Hybrid Nanofluid Inside a Novel Oval-Shaped Annulus Enclosure," *Case Studies in Thermal Engineering*, vol. 61, pp. 1-27, 2024. [CrossRef] [Google Scholar] [Publisher Link]

[4] Muhammad Mahmood Aslam Bhutta et al., "CFD Applications in Various Heat Exchanger Designs: A Review," *Applied Thermal Engineering*, vol. 32, pp. 1-12, 2012. [CrossRef] [Google Scholar] [Publisher Link]

[5] Jihyeok Choi et al., "Combination of Computational Fluid Dynamics and Design of Experiments to Optimize Modules for Direct Contact Membrane Distillation," *Desalination*, vol. 524, 2022. [CrossRef] [Google Scholar] [Publisher Link]

[6] Hanane Dagdougui et al., "Thermal Analysis and Performance Optimization of a Solar Water Heater Flat Plate Collector: Application to Tetouan (Morocco)," *Renewable and Sustainable Energy Reviews*, vol. 15, no. 1, pp. 630-638, 2011. [CrossRef] [Google Scholar] [Publisher Link]

[7] Tiko Rago Desisa, "Experimental and Numerical Investigation of Heat Transfer Characteristics in Solar Flat Plate Collector using Nanofluids," *International Journal of Thermofluids*, vol. 18, pp. 1-11, 2023. [CrossRef] [Google Scholar] [Publisher Link]

[8] Alexander I.J. Forrester, András Sóbester, and Andy J. Keane, *Engineering Design Via Surrogate Modelling: A Practical Guide*, John Wiley & Sons, 2008. [CrossRef] [Google Scholar] [Publisher Link]

[9] Celine Garnier, Tariq Muneer, and John Currie, "Numerical and Empirical Evaluation of a Novel Building Integrated Collector Storage Solar Water Heater," *Renewable Energy*, vol. 126, pp. 281-295, 2018. [CrossRef] [Google Scholar] [Publisher Link]

[10] Jiawei Gong, and Krishnan Sumathy, "9 - Active Solar Water Heating Systems," *Advances in Solar Heating and Cooling*, pp. 203-224, 2016. [CrossRef] [Google Scholar] [Publisher Link]

[11] Dawit Gudeta Gunjo, Pinakeswar Mahanta, and Puthuveettil Sreedharan Robi, "CFD And Experimental Investigation of Flat Plate Solar Water Heating System Under Steady-State Condition," *Renewable Energy*, vol. 106, pp. 24-36, 2017. [CrossRef] [Google Scholar] [Publisher Link]

[12] Ali S.Hussen, and Balewgize Amare Zeru, "Design, Optimization and CFD Simulation of Solar Air Heater with Jet Impingement on V-Corrugated Plate," *International Research Journal of Engineering and Technology (IRJET)*, vol. 7, no. 5, pp. 1805-1813, 2020. [Google Scholar] [Publisher Link]

[13] Subramanian Jaisankar et al., "A Comprehensive Review on Solar Water Heaters," *Renewable and Sustainable Energy Reviews*, vol. 15, no. 6, pp. 3045-3050, 2011. [CrossRef] [Google Scholar] [Publisher Link]

[14] Mohammed Abdul Junaid et al., "Thermal Analysis of Solar Flat Plate Collector using CFD," *International Journal of Engineering Research and Technology (IJERT)*, vol. 6, no. 4, pp. 659-662, 2017. [CrossRef] [Google Scholar] [Publisher Link]

[15] Soteris A. Kalogirou, "Solar Thermal Collectors and Applications," *Progress in Energy and Combustion Science*, vol. 30, no. 3, pp. 231-295, 2004. [CrossRef] [Google Scholar] [Publisher Link]

[16] Arash Kazemian et al., "Optimizing Photovoltaic Thermal Systems with Wavy Collector Tube: A Response Surface-based Design Study with Desirability Analysis," *Applied Thermal Engineering*, vol. 258, pp. 1-62, 2025. [CrossRef] [Google Scholar] [Publisher Link]

[17] V.S. Korpale et al., "Numerical Simulations and Optimization of Solar Air Heaters," *Applied Thermal Engineering*, vol. 180, 2020. [CrossRef] [Google Scholar] [Publisher Link]

[18] Korti Mohammed Choukri et al., "Optimizing Solar Water Heater Performance Through a Numerical Study of Zig-Zag Shaped Tubes," *Thermal Science*, vol. 27, no. 4, pp. 3143-3153, 2023. [CrossRef] [Google Scholar] [Publisher Link]

[19] Rohit Kumar, and Ram Gopal Verma, "Enhancing Solar Water Heater Performance Through ANSYS FLUENT: An Exploratory and Numerical Analysis," *International Journal of Engineering, Science and Mathematics*, vol. 12, no. 7, pp. 1-11, 2023. [Google Scholar] [Publisher Link]

[20] William L. Oberkampf et al., *Verification and Validation in Scientific Computing*, 2nd ed., Cambridge University Press, 2010. [Google Scholar] [Publisher Link]

[21] Eghosa Omo-oghogho, and Sufianu Adeiza Alıu, "Modelling of a Flat Plate Solar Collector System using Response Surface Methodology," *Black Sea Journal of Engineering and Science*, vol. 3, no. 3, pp. 89-97, 2020. [CrossRef] [Google Scholar] [Publisher Link]

[22] Krishna Murari Pandey, and Rajesh Chaurasiya, "A Review on Analysis and Development of Solar Flat Plate Collectors," *Renewable and Sustainable Energy Reviews*, vol. 67, pp. 641-650, 2017. [CrossRef] [Google Scholar] [Publisher Link]

[23] Zvawanda Paul, and Peace-Maker Masukume, "Efficiency Optimization in Solar Water Heaters: A Comparative CFD Study of Design Configurations," *Power Engineering and Engineering Thermophysics*, vol. 2, no. 4, pp, 238-249, 2023. [CrossRef] [Google Scholar] [Publisher Link]

[24] M.S.W. Potgieter, Christiaan R. Bester, and Muaaz Bhamjee, "Experimental and CFD Investigation of a Hybrid Solar Air Heater," *Solar Energy*, vol. 195, pp. 413-428, 2020. [CrossRef] [Google Scholar] [Publisher Link]

[25] Bose Prabhu et al., "Comprehensive Energy and Enviro-Economic Performance Analysis of a Flat Plate Solar Water Heater with a Modified Absorber," *Thermal Science and Engineering Progress*, vol. 54, 2024. [CrossRef] [Google Scholar] [Publisher Link]

[26] Bootan S. Qader et al., "RSM Approach for Modelling and Optimization of Designing Parameters for Inclined Fins of Solar Air Heater," *Renewable Energy*, vol. 136, pp. 48-68, 2019. [CrossRef] [Google Scholar] [Publisher Link]

[27] Ch. Reichl et al., "Comparison of Modelled Heat Transfer and Fluid Dynamics of a Flat Plate Solar Air Heating Collector Towards Experimental Data," *Solar Energy*, vol. 120, pp. 450-463, 2015. [CrossRef] [Google Scholar] [Publisher Link]

[28] S. Sadhishkumar, and Thangavel Balusamy, "Performance Improvement in Solar Water Heating Systems - A Review," *Renewable and Sustainable Energy Reviews*, vol. 37, pp. 191-198, 2014. [CrossRef] [Google Scholar] [Publisher Link]

[29] R. Soundararajan et al., "Design and Optimization of Solar Water Heater using CFD Analysis," *International Journal of Research in Advent Technology*, vol. 3, no. 4, pp. 107-110, 2015. [Publisher Link]

[30] Runsheng Tang, Yuqin Yang, and Wenfeng Gao, "Comparative Studies on Thermal Performance of Water-In-Glass Evacuated Tube Solar Water Heaters with Different Collector Tilt Angles," *Solar Energy*, vol. 85, no. 7, pp. 1381-1389, 2011. [CrossRef] [Google Scholar] [Publisher Link]

[31] Sabaa Theeyzen, and Basim Freegah, "The Effect of Added Wire Mesh on the Thermal Efficiency of the Flat Plate Solar Water Heater Collector," *Results in Engineering*, vol. 24, pp. 1-12, 2024. [CrossRef] [Google Scholar] [Publisher Link]

[32] R. Thejaraju et al., "CFD Analysis of Solar Flat Plate Collector with Semi-Circular Baffles," *International Journal of Mechanical and Production Engineering*, vol. 5, no. 5, pp. 105-109, 2017. [Google Scholar] [Publisher Link]

[33] Vineet Veer Tyagi, and D. Buddhi, "PCM Thermal Storage in Buildings: A State-of-the-Art," *Renewable and Sustainable Energy Reviews*, vol. 11, no. 6, pp. 1146-1166, 2007. [CrossRef] [Google Scholar] [Publisher Link]

[34] Poornodaya Venkata Krishna Varma Kola et al., "Optimization of Performance Parameters of a Double Pipe Heat Exchanger with Cut Twisted Tapes using CFD and RSM," *Chemical Engineering and Processing: Process Intensification*, vol. 163, 2021. [CrossRef] [Google Scholar] [Publisher Link]

[35] Elumalai Vengadesan, and Ramalingam Senthil, "A Review on Recent Development of Thermal Performance Enhancement Methods of Flat Plate Solar Water Heater," *Solar Energy*, vol. 206, pp. 935-961, 2020. [CrossRef] [Google Scholar] [Publisher Link]

[36] Gaurav Vyas, Raja Sekhar Dondapati, and Sudhanshu Dogra, "Thermal Efficiency Augmentation of Flat Solar Water Heater using Nanoparticles for Sustainable use in Industries," *Materials Today: Proceedings*, 2024. [CrossRef] [Google Scholar] [Publisher Link]

[37] Ye Wang et al., "Multi-Objective Optimization Design of Solar Air Collector with a Frustum-Shaped Protrusion," *Solar Energy*, vol. 267, 2024. [CrossRef] [Google Scholar] [Publisher Link]

[38] Samer Yassin Alsadi, and Tareq Foqha, "Mass Flow Rate Optimization of Solar Heating Systems based on Flat Plate Solar Collectors: A Case Study," *World Journal of Advanced Research and Reviews*, vol. 12, no. 3, pp. 61-71, 2021. [CrossRef] [Google Scholar] [Publisher Link]

[39] Lemi Negera Woyessa et al., "Design and CFD Simulation of Solar Water Heater used in Solar-Assisted Biogas System," *International Journal of Innovative Technology and Exploring Engineering*, vol. 9, no. 3, pp. 371-380, 2020. [CrossRef] [Google Scholar] [Publisher Link]

[40] Y.P. Yadav, and Gopal Nath Tiwari, "Large Scale Solar Water Heater: Experimental and Theoretical Studies," *Energy Conversion and Management*, vol. 31. no. 4, pp. 337-351, 1991. [CrossRef] [Google Scholar] [Publisher Link]

[41] Mohammed Yunus, and Mohammad S. Alsoufi, "Multi-Thermal Performance Optimization of Semi-Circular Heat Pipes Integrated with Various Solar Collector Profiles," *Renewables: Wind, Water, and Solar*, vol. 8, no. 1, pp. 1-17, 2021. [CrossRef] [Google Scholar] [Publisher Link]